Numerical Solutions for Fractional Multi-Group Neutron Diffusion System of Equations

Mohammed Shqair[1], **Iqbal M. Batiha**[2,3*], **Mohammed H. E. Abu-Sei'leek**[1], **Shameseddin Alshorm**[2], **Amira Abdelnebi**[4], **Iqbal H. Jebril**[2], **S. A. Abd El-Azeem**[5,6]

[1]Faculty of Science, Zarqa University, Zarqa 13110, Jordan
[2]Department of Mathematics, Al Zaytoonah University, Amman 11733, Jordan
[3]Nonlinear Dynamics Research Center (NDRC), Ajman University, Ajman 346, UAE
[4]Laboratory of pure and applied mathematics, University of Mostaganem, Mostaganem 27000, Algeria
[5]Physics Department, College of Sciences and Humanities, Prince Sattam Bin Abdulaziz University, Al-Kharj 11942, Saudi Arabia
[6]Physics Department, Faculty of Women for Arts, Science and Education, Ain Shams University, Cairo 11757, Egypt

Emails: shqeeeer@gmail.com; i.batiha@zuj.edu.jo; mseileek@zu.edu.jo; alshormanshams@gmail.com; amira.math27@gmail.com; i.jebril@zuj.edu.jo; samah.zy2@gmail.com

Abstract

This paper addresses fractional-order versions of multi-group neutron diffusion systems of equations, focusing on two numerical solutions. First, it employs the Laplace transform method to solve the classical version of multi-group neutron diffusion equations. Subsequently, it transforms these equations into their corresponding fractional-order versions using the Caputo differentiator. To handle the resultant fractional-order system, a novel approach is introduced to reduce it from a system of 2α-order to a system of α-order. This converted system is then solved using the so-called Modified Fractional Euler Method (MFEM). As far as we know, this is the first time that such numerical schemes have been used to deal with the systems at hand. The paper covers the multi-group neutron diffusion equations in spherical, cylindrical, and slab reactors, all solved and converted for verification purposes.

Keywords: multi-group neutron diffusion equations; Laplace transform method; fractional calculus; modified fractional Euler method.

1 Introduction

The dispersion of neutrons within the reactor are one of the fundamental processes that control how the core of a nuclear reactor behaves. The neutron balancing equation, often known as the neutron transport equation, is the foundation for the mathematical description of a neutron distribution. In truth, the transport equation is complex and the only physical models for which accurate solutions have been obtained thus far.[1,2] The neutron transport equation can be simplified into neutron diffusion equations using Fick's law. These equations describe the various velocities of neutrons in a reactor and categorize them by energy levels to model neutron behavior.[3–8] In multi-group neutron diffusion equations, the influence of multiple energy-level interactions on neutron behavior is considered. Solving these equations allows engineers to ensure reactor criticality, maintaining a controlled and self-sustaining chain reaction within the nuclear reactor.[9–13] Factors such as fuel composition, reactor design, and control rod positions are considered for a comprehensive understanding and regulation of the process.[14–19]

https://doi.org/10.54216/IJNS.240401

Received: September 25, 2023 Revised: February 19, 2024 Accepted: May 07, 2024

In nuclear reactor physics, cross-sections are fundamental for assessing the likelihood of specific nuclear reactions. Cross-section (σ) represents the effective size of a target nucleus, indicating the probability of nuclear interactions when particles like neutrons interact with nuclei. Various types of nuclear processes have associated cross-sections. Fission Cross Section (σ_f) measures the likelihood of a nucleus splitting when interacting with a neutron. It's crucial for understanding and controlling nuclear fission, the process where a heavy nucleus breaks into lighter nuclei, releasing energy and additional neutrons. Another important cross-section is the absorption cross-section (σ_a) which indicates the probability of a nucleus absorbing a neutron without undergoing fission. Neutron capture by the nucleus, explained by the absorption cross-section, leads to the creation of heavier isotopes, or initiates different nuclear processes. This process is essential for regulating reactor reactivity and neutron populations. Additionally, the radiative capture cross-section (σ_y) quantifies the probability of a nucleus capturing a neutron and then emitting a gamma-ray photon. This process occurs when a nucleus absorbs a neutron and transitions to a higher energy state, releasing energy in the form of gamma-ray radiation. In a nuclear reactor, radiation capture plays a crucial role in both the creation of radioactive isotopes and the generation of energy, significantly impacting reactor operations and outcomes.[20,21]

This study initially presents an approach utilizing the Laplace Transform Method (LTM) to offer a numerical solution for the classical multi-group neutron diffusion equations in various geometric shapes, including slab, cylindrical, and spherical configurations. The LTM is an efficient method that enables the solution of these equations without the need for discretization, perturbation, or linearization techniques. Instead, it constructs an approximate, practical and effective solution for addressing complex neutron diffusion problems. Also, this paper employs techniques to convert higher-order differential equations into first-order ones in the context of Fractional Differential Equations (FDEs). The process involves introducing new variables and transforming the equation into a system of interconnected α-order differential equations, where $0 < \alpha \leq 1$. The transformed α-order system can then be tackled with one of powerful methods for dealing with fractional-order systems, called the Modified Fractional Euler Method (MFEM). A recent advancement, the MFEM, has shown efficacy in solving systems with fractional calculus of order α. This paper employs MFEM to address fractional multi-group neutron diffusion equations.[22–28]

2 Preliminary concepts

In this section, we will introduce fundamental definitions and theorems related to fractional calculus, including the Riemann-Liouville integral and derivative, the Caputo derivative and other relevant concepts.[29–3224,33] The fractional Riemann-Liouville integral of a function f of order $\alpha > 0$ is initially defined by

$$J^{\alpha} f(t) = \frac{1}{\Gamma(\alpha)} \int_0^t f(\tau)(t-\tau)^{\alpha-1}\, d\tau, \quad t > 0,\ \alpha > 0. \tag{1}$$

Some of the properties of the Riemann-Liouville integral are given below for completeness:[24,33]

$$J^0 f(t) = f(t). \tag{2}$$

$$J^{\alpha}(t-a)^{\gamma} = \frac{\Gamma(\gamma+1)}{\Gamma(\alpha+\gamma+1)}(t-a)^{\alpha+\gamma}, \quad \gamma \geq -1, a \in \mathbb{R}. \tag{3}$$

$$J^{\alpha} J^{\beta} f(t) = J^{\beta} J^{\alpha} f(t), \quad \alpha, \beta \geq 0. \tag{4}$$

$$J^{\alpha} J^{\beta} f(t) = J^{\alpha+\beta} f(t), \quad \alpha, \beta \geq 0. \tag{5}$$

[24,33] Let m be the smaller number greater than α. The Caputo fractional derivative of order $\alpha > 0$ is defined as

$$D^{\alpha} f(t) = \begin{cases} \frac{1}{\Gamma(m-\alpha)} \int_0^t (t-\tau)^{-\alpha+m-1} \frac{d^m f(\tau)}{d\tau^m}\, d\tau, & m-1 < \alpha < m, \\ \frac{d^m f(t)}{dt^m}, & \alpha = m, \end{cases} \tag{6}$$

where $m \in \mathbb{N}$, $t > 0$ and f is a real-valued function. Some of the characteristics of the Caputo derivative are listed below:[33]

1. $D^{\alpha} c = 0$, where c is constant.

https://doi.org/10.54216/IJNS.240401

Received: September 25, 2023 Revised: February 19, 2024 Accepted: May 07, 2024

2. For $a \in \mathbb{R}$ we have

$$D^{\alpha}(t-a)^{\rho} = \begin{cases} \frac{\Gamma(\rho+1)}{\Gamma(\rho-\alpha+1)}(t-a)^{\rho-\alpha}, & \rho > \alpha - 1, \\ 0, & otherwise. \end{cases} \tag{7}$$

3. D^{α} is a linear operator, i.e.,

$$D^{\alpha}(\mu f(t) + \omega k(t)) = \mu D^{\alpha} f(t) + \omega D^{\alpha} k(t),$$

where μ and ω are constants.

4. The semigroup property holds,[34] i.e.

$$D^{\alpha} D^{\beta} f(t) = D^{\alpha+\beta} f(t), \tag{8}$$

under the additional assumption that $f^{(1)}(0) = 0$ in the case $\alpha + \beta > 1$.

In addition, we need to recall the following basic property. If $m - 1 < \alpha \leq m$, $m \in \mathbb{N}^*$, then we have

$$J^{\alpha} D^{\alpha} f(t) = f(t) - \sum_{i=1}^{m} f^{i}(0^{+}) \frac{t^{i}}{i!}, \;\; t > 0. \tag{9}$$

Theorem 2.1. [35] *[Generalized Taylor's formula] Suppose that $D^{k\alpha} f(x) \in C(0, b]$ for $k = 0, 1, 2, \cdots, n+1$, where $0 < \alpha \leq 1$. Then we can expand the function f about the node x_0 as follows:*

$$f(x) = \sum_{i=0}^{n} \frac{(x - x_0)^{i\alpha}}{\Gamma(i\alpha + 1)} (D^{i\alpha} f)(x_0) + \frac{(x - x_0)^{(n+1)\alpha}}{\Gamma((n+1)\alpha + 1)} (D^{(n+1)\alpha} f)(\xi), \tag{10}$$

with $0 < \xi < x$, $\forall x \in (0, b]$.

[36] Let function f be defined on $[0, \infty)$. Then Laplace transform $\mathscr{L}\{f\}$ is another function $F(s)$, which is defined as

$$F(s) = \mathscr{L}\{f\} := \int_{0}^{\infty} e^{-st} f(t) dt. \tag{11}$$

Remark 2.2. Some properties of Laplace transform are listed below for completeness:[36]

$$\begin{aligned} &\mathscr{L}\{ty\} = -\frac{d}{ds}\mathscr{L}\{y\}. \\ &\mathscr{L}\{f'(t)\} = -f(0^{+}) + s\mathscr{L}\{f\} = sF(s) - f(0^{+}). \\ &\mathscr{L}\{f''(t)\} = s^{2}F(s) - sf(0^{+}) - f'(0^{+}). \end{aligned}$$

3 Theoretical framework on multi-group neutron diffusion system

In this section, we intend first to recall the general form of the multi-group neutron diffusion system. Then we will convert this system of multi-group neutron diffusion system into its fractional-order form.

3.1 Classical form of multi-group neutron diffusion system

It is assumed that the multi-group neutron diffusion equations system has a single solution in the interval of integration with the following form:[6,20]

$$\begin{aligned}
&\nabla^2\phi_1(r) + C_{11}\phi_1(r) + C_{12}\phi_2(r) + C_{13}\phi_3(r) + \cdots + C_{1n}\phi_n(r) = 0,\\
&\nabla^2\phi_2(r) + C_{21}\phi_1(r) + C_{22}\phi_2(r) + C_{23}\phi_3(r) + \cdots + C_{2n}\phi_n(r) = 0,\\
&\nabla^2\phi_3(r) + C_{31}\phi_1(r) + C_{32}\phi_2(r) + C_{33}\phi_3(r) + \cdots + C_{3n}\phi_n(r) = 0,\\
&\vdots\\
&\nabla^2\phi_n(r) + C_{n1}\phi_1(r) + C_{n2}\phi_2(r) + C_{n3}\phi_3(r) + \cdots + C_{nn}\phi_n(r) = 0,
\end{aligned} \tag{12}$$

for which the constants C_{ii}, C_{ij} and D_i are defined as follows:

$$\begin{aligned}
C_{ii} &= \frac{x_i v_i \sum_{i=1}^{n} f_i - \left(\sum_{i=1}^{n}\gamma_i + \sum_{i=1}^{n}\sum_{j=1}^{n} s_{ij}\right)}{D_i},\\
C_{ij} &= \frac{\sum_{i=1}^{n}\sum_{j=1} s_{ij} + x_i v_j \sum_{i=1}^{n} f_i}{D_i},\\
D_i &= \frac{1}{3\left(\sum_{i=1}^{n} f_i + \sum_{i=1}^{n} s_{ii} + \sum_{i=1}^{n}\sum_{j=1} s_{ij} + \sum_{i=1}^{n}\gamma_i\right)},
\end{aligned} \tag{13}$$

where D_i is a group diffusion coefficient and γ_i is the macroscopic radiative capture cross-section, which represents the probability of a nucleus capturing a neutron and emitting a gamma-ray photon. Herein, the function $\phi_i(r)$ is assumed to be an analytic function for adapting some essential needs, especially the semigroup property reported in (8), for $i = 1, 2, 3, \cdots, n$.

The constants in (13) are typically defined in terms of different macroscopic cross-sections, the number of neutrons produced per fission for each group (v_i), and the fraction of fission neutrons that are emitted with energies in the i^{th}-group (x_i). The above system of equations describes the behavior of the neutrons in nuclear reactors where each flux ϕ_i expresses the neutron flux with a specific speed. Each flux reaches its maximum at the center of the reactor; its derivative vanishes, so the initial conditions can be written as

$$\phi_i(0) = h_i, \phi_i^{'}(0) = 0, i = 1, 2, \cdots, n, \tag{14}$$

where the fluxes $\phi_i(r)$ are functions of independent variable r and $h_i \in \mathbb{R}$, $\forall i = 1, 2, \cdots, n$. Throughout this work, it is assumed that $\phi_i(r)$ are analytic functions for $r \geq 0$, $\forall i = 1, 2, \cdots, n$. The multi-group time-independent neutron diffusion system have three nuclear reactor essential geometries, namely spherical, cylindrical and slab reactors which will be studied respectively. In the following content, we will discuss these three cases in terms of finding their solutions by using LTM.

3.1.1 Multi-group neutron diffusion system in spherical reactor

A type of nuclear reactor design known as a multi-group neutron diffusion system in spherical reactor (MG-SR) makes use of several energy groups to simulate the behavior of neutrons inside the reactor core. It is a variant of reactor analysis's more widely used multi-group neutron diffusion theory. The energy spectrum of neutrons in a MEG-SR is split into a number of distinct energy groups. A set of diffusion equations approximates the neutron behavior inside each energy group, which represents a particular range of neutron energies. The multi-group neutron diffusion system in spherical reactor can be express as

$$\begin{aligned}
&r\phi_1^{''}(r) + 2\phi_1^{'}(r) + rC_{11}\phi_1(r) + rC_{12}\phi_2(r) + rC_{13}\phi_3(r) + \cdots + rC_{1n}\phi_n(r) = 0\\
&r\phi_2^{''}(r) + 2\phi_2^{'}(r) + rC_{21}\phi_1(r) + rC_{22}\phi_2(r) + rC_{23}\phi_3(r) + \cdots + rC_{2n}\phi_n(r) = 0\\
&r\phi_3^{''}(r) + 2\phi_3^{'}(r) + rC_{31}\phi_1(r) + rC_{32}\phi_2(r) + rC_{33}\phi_3(r) + \cdots + rC_{3n}\phi_n(r) = 0\\
&\vdots\\
&r\phi_n^{''}(r) + 2\phi_n^{'}(r) + rC_{n1}\phi_1(r) + rC_{n2}\phi_2(r) + rC_{n3}\phi_3(r) + \cdots + rC_{nn}\phi_n(r) = 0,
\end{aligned} \tag{15}$$

Received: September 25, 2023 Revised: February 19, 2024 Accepted: May 07, 2024

with the following initial conditions:

$$\begin{aligned} &\phi_i(0^+) = a_i,\ i = 1, 2, \cdots, n. \\ &\phi_i^{'}(0^+) = b_i,\ i = 1, 2, \cdots, n. \end{aligned} \tag{16}$$

To deal with such a system with the use of LTM, we take the Laplace transform of the both sides of the above system to get

$$\begin{aligned} &\mathscr{L}(r\phi_1^{''}(r)) + 2\mathscr{L}(\phi_1^{'}(r))) + C_{11}\mathscr{L}(r\phi_1(r)) + C_{12}\mathscr{L}(r\phi_2(r)) + \cdots + C_{1n}\mathscr{L}(r\phi_n(r)) = 0, \\ &\mathscr{L}(r\phi_2^{''}(r)) + 2\mathscr{L}(\phi_2^{'}(r))) + C_{21}\mathscr{L}(r\phi_1(r)) + C_{22}\mathscr{L}(r\phi_2(r)) + \cdots + C_{2n}\mathscr{L}(r\phi_n(r)) = 0, \\ &\mathscr{L}(r\phi_3^{''}(r)) + 2\mathscr{L}(\phi_3^{'}(r))) + C_{31}\mathscr{L}(r\phi_1(r)) + C_{32}\mathscr{L}(r\phi_2(r)) + \cdots + C_{3n}\mathscr{L}(r\phi_n(r)) = 0, \\ &\vdots \\ &\mathscr{L}(r\phi_n^{''}(r)) + 2\mathscr{L}(\phi_n^{'}(r))) + C_{n1}\mathscr{L}(r\phi_1(r)) + C_{n2}\mathscr{L}(r\phi_2(r)) + \cdots + C_{nn}\mathscr{L}(r\phi_n(r)) = 0. \end{aligned} \tag{17}$$

By using Remark 2.2, we can get

$$\begin{aligned} &\frac{-d}{ds}(s^2\mathscr{L}\{\phi_1(r)\} - s\phi_1(0^+) - \phi_1^{'}(0^+)) + 2(s\mathscr{L}\{\phi_1(r)\} - \phi_1(0^+)) + C_{11}(\frac{-d}{ds}\mathscr{L}\{\phi_1(r)\}) \\ &+ C_{12}(\frac{-d}{ds}\mathscr{L}\{\phi_2(r)\}) + C_{13}(\frac{-d}{ds}\mathscr{L}\{\phi_3(r)\}) + \cdots + C_{1n}(\frac{-d}{ds}\mathscr{L}\{\phi_n(r)\}) = 0, \\ &\frac{-d}{ds}(s^2\mathscr{L}\{\phi_2(r)\} - s\phi_2(0^+) - \phi_2^{'}(0^+)) + 2(s\mathscr{L}\{\phi_2(r)\} - \phi_2(0^+)) + C_{21}(\frac{-d}{ds}\mathscr{L}\{\phi_1(r)\}) \\ &+ C_{22}(\frac{-d}{ds}\mathscr{L}\{\phi_2(r)\}) + C_{23}(\frac{-d}{ds}\mathscr{L}\{\phi_3(r)\}) + \cdots + C_{2n}(\frac{-d}{ds}\mathscr{L}\{\phi_n(r)\}) = 0, \\ &\frac{-d}{ds}(s^2\mathscr{L}\{\phi_3(r)\} - s\phi_3(0^+) - \phi_3^{'}(0^+)) + 2(s\mathscr{L}\{\phi_3(r)\} - \phi_3(0^+)) + C_{31}(\frac{-d}{ds}\mathscr{L}\{\phi_1(r)\}) \\ &+ C_{32}(\frac{-d}{ds}\mathscr{L}\{\phi_2(r)\}) + C_{33}(\frac{-d}{ds}\mathscr{L}\{\phi_3(r)\}) + \cdots + C_{3n}(\frac{-d}{ds}\mathscr{L}\{\phi_n(r)\}) = 0 \\ &\vdots \\ &\frac{-d}{ds}(s^2\mathscr{L}\{\phi_n(r)\} - s\phi_n(0^+) - \phi_n^{'}(0^+)) + 2(s\mathscr{L}\{\phi_n(r)\} - \phi_n(0^+)) + C_{n1}(\frac{-d}{ds}\mathscr{L}\{\phi_1(r)\}) \\ &+ C_{n2}(\frac{-d}{ds}\mathscr{L}\{\phi_2(r)\}) + C_{n3}(\frac{-d}{ds}\mathscr{L}\{\phi_3(r)\}) + \cdots + C_{nn}(\frac{-d}{ds}\mathscr{L}\{\phi_n(r)\}) = 0. \end{aligned} \tag{18}$$

With the help of assuming $\mathscr{L}\{\phi_i(r)\}) = T_i(s)$, for all $i = 1, 2, \cdots, n$, we get:

$$\begin{aligned} &\frac{-d}{ds}(s^2T_1(s) - a_1s - b_1) + 2(sT_1(s) - a_1) - C_{11}T_1^{'}(s) - C_{12}T_2^{'}(s) - C_{13}T_3^{'}(s) - \cdots - C_{1n}T_n^{'}(s) = 0, \\ &\frac{-d}{ds}(s^2T_2(s) - a_2s - b_2) + 2(sT_2(s) - a_2) - C_{21}T_1^{'}(s) - C_{22}T_2^{'}(s) - C_{23}T_3^{'}(s) - \cdots - C_{2n}T_n^{'}(s) = 0, \\ &\frac{-d}{ds}(s^2T_3(s) - a_3s - b_3) + 2(sT_3(s) - a_3) - C_{31}T_1^{'}(s) - C_{32}T_2^{'}(s) - C_{33}T_3^{'}(s) - \cdots - C_{3n}T_n^{'}(s) = 0, \\ &\vdots \\ &\frac{-d}{ds}(s^2T_n(s) - a_ns - b_n) + 2(sT_n(s) - a_n) - C_{n1}T_1^{'}(s) - C_{n2}T_2^{'}(s) - C_{n3}T_3^{'}(s) - \cdots - C_{nn}T_n^{'}(s) = 0. \end{aligned} \tag{19}$$

By simplifying the previous system (19), we get

$$\begin{aligned} &-(s^2 + C_{11})T_1^{'}(s) - C_{12}T_2^{'}(s) - C_{13}T_3^{'}(s) - \cdots - C_{1n}T_n^{'}(s) = a_1, \\ &-C_{21}T_1^{'}(s) - (s^2 + C_{22})T_2^{'}(s) - C_{23}T_3^{'}(s) - \cdots - C_{2n}T_n^{'}(s) = a_2, \\ &-C_{31}T_1^{'}(s) - C_{32}T_2^{'}(s) - (s^2 + C_{33})T_3^{'}(s) - \cdots - C_{3n}T_n^{'}(s) = a_3, \\ &\vdots \\ &-C_{n1}T_1^{'}(s) - C_{n2}T_2^{'}(s) - C_{n3}T_3^{'}(s) - \cdots - (s^2 + C_{nn})T_n^{'}(s) = a_n. \end{aligned} \tag{20}$$

Received: September 25, 2023 Revised: February 19, 2024 Accepted: May 07, 2024

The matrix general form is then as follows:

$$\begin{bmatrix} -(s^2+C_{11})-C_{12}-C_{13}-\cdots-C_{1n} \\ -C_{21}-(s^2+C_{22})-C_{23}-\cdots-C_{2n} \\ -C_{31}-C_{32}-(s^2+C_{33})-\cdots-C_{3n} \\ \vdots \\ -C_{n1}-C_{n2}-C_{n3}-\cdots-(s^2+C_{nn}) \end{bmatrix} \begin{bmatrix} T_1^{'}(s) \\ T_2^{'}(s) \\ T_3^{'}(s) \\ \vdots \\ T_n^{'}(s) \end{bmatrix} = \begin{bmatrix} a_1 \\ a_2 \\ a_2 \\ \vdots \\ a_n \end{bmatrix}. \tag{21}$$

Note that $A(s)$, T and K are defined as follow:

$$A(s) = \begin{bmatrix} -(s^2+C_{11})-C_{12}-C_{13}-\cdots-C_{1n} \\ -C_{21}-(s^2+C_{22})-C_{23}-\cdots-C_{2n} \\ -C_{31}-C_{32}-(s^2+C_{33})-\cdots-C_{3n} \\ \vdots \\ -C_{n1}-C_{n2}-C_{n3}-\cdots-(s^2+C_{nn}) \end{bmatrix}, T^{'}(s) = \begin{bmatrix} T_1^{'}(s) \\ T_2^{'}(s) \\ T_3^{'}(s) \\ \vdots \\ T_n^{'}(s) \end{bmatrix}, K = \begin{bmatrix} a_1 \\ a_2 \\ a_2 \\ \vdots \\ a_n \end{bmatrix}. \tag{22}$$

By using the previous assumptions, we can write system (21) as $A(s)T^{'}(s) = K$. Also, if $A(s)$ is invertible, we can write it as follow

$$T^{'}(s) = A^{-1}(s)K. \tag{23}$$

System (23) can be then solved numerically by using a prepared MATLAB code with noting that $\phi_i(r) = \mathscr{L}^{-1}\{T_i(s)\}$, for all $i = 1, 2, \cdots, n$. This would give the solution $\phi_i(r)$ of system (15). In fact, such a system's solution makes it evident that the scheme provided to generate system (23) is convergent, and this what we will see in Section 4. In particular, if the functions $T_i(s)$ have Laplace transforms $\phi_i(r)$, for all $i = 1, 2, \cdots, n$, then for the inverse Laplace transform to exist, the integral

$$\phi_i(r) = \frac{1}{2\pi j} \lim_{N\to\inf} \int_{\delta-jN}^{\delta+jN} T(s)e^{st}ds$$

must converge, where δ is a real constant such that the contour of integration lies to the right of all singularities $T(s)$.

3.1.2 Multi-group neutron diffusion system in cylindrical reactor

The multi-group neutron diffusion system in a cylindrical reactor will be solved here by using LTM as well. Such a system has the form

$$\begin{aligned} & r\phi_1^{''}(r) + \phi_1^{'}(r) + r\Big(C_{11}\phi_1(r) + C_{12}\phi_2(r) + C_{13}\phi_3(r) + \cdots + C_{1n}\phi_n(r)\Big) = 0, \\ & r\phi_2^{''}(r) + \phi_2^{'}(r) + r\Big(C_{21}\phi_1(r) + C_{22}\phi_2(r) + C_{23}\phi_3(r) + \cdots + C_{2n}\phi_n(r)\Big) = 0, \\ & r\phi_3^{''}(r) + \phi_3^{'}(r) + r\Big(C_{31}\phi_1(r) + C_{32}\phi_2(r) + C_{33}\phi_3(r) + \cdots + C_{3n}\phi_n(r)\Big) = 0, \\ & \vdots \\ & r\phi_n^{''}(r) + \phi_n^{'}(r) + r\Big(C_{n1}\phi_1(r) + C_{n2}\phi_2(r) + C_{n3}\phi_3(r) + \cdots + C_{nn}\phi_n(r)\Big) = 0, \end{aligned} \tag{24}$$

with the following initial conditions:

$$\phi_i(0^+) = a_i,\ \phi_i^{'}(0^+) = b_i,\ \text{for all } i = 1, 2, \cdots, n. \tag{25}$$

https://doi.org/10.54216/IJNS.240401

Received: September 25, 2023 Revised: February 19, 2024 Accepted: May 07, 2024

By taking the Laplace transform of the both sides of the above system and by using the same manner of the spherical case, we obtain

$$\begin{aligned}
&-(s^2+C_{11})T_1^{'}(s)-C_{12}T_2^{'}(s)-C_{13}T_3^{'}(s)-\cdots-C_{1n}T_n^{'}(s)=sT_1(s),\\
&-C_{21}T_1^{'}(s)-(s^2+C_{22})T_2^{'}(s)-C_{23}T_3^{'}(s)-\cdots-C_{2n}T_n^{'}(s)=sT_2(s),\\
&-C_{31}T_1^{'}(s)-C_{32}T_2^{'}(s)-(s^2+C_{33})T_3^{'}(s)-\cdots-C_{3n}T_n^{'}(s)=sT_3(s),\\
&\vdots\\
&-C_{n1}T_1^{'}(s)-C_{n2}T_2^{'}(s)-C_{n3}T_3^{'}(s)-\cdots-(s^2+C_{nn})T_n^{'}(s)=sT_n(s).
\end{aligned} \tag{26}$$

The matrix general form will then be as follows:

$$\begin{bmatrix} -(s^2+C_{11})-C_{12}-C_{13}-\cdots-C_{1n}\\ -C_{21}-(s^2+C_{22})-C_{23}-\cdots-C_{2n}\\ -C_{31}-C_{32}-(s^2+C_{33})-\cdots-C_{3n}\\ \vdots\\ -C_{n1}-C_{n2}-C_{n3}-\cdots-(s^2+C_{nn}) \end{bmatrix} \begin{bmatrix} T_1^{'}(s)\\ T_2^{'}(s)\\ T_3^{'}(s)\\ \vdots\\ T_n^{'}(s) \end{bmatrix} = s\begin{bmatrix} T_1(s)\\ T_2(s)\\ T_3(s)\\ \vdots\\ T_n(s) \end{bmatrix}. \tag{27}$$

Note that $A(s)$, $T^{'}(s)$ and $T(s)$ will be defined as follow:

$$A(s)=\begin{bmatrix} -(s^2+C_{11})-C_{12}-C_{13}-\cdots-C_{1n}\\ -C_{21}-(s^2+C_{22})-C_{23}-\cdots-C_{2n}\\ -C_{31}-C_{32}-(s^2+C_{33})-\cdots-C_{3n}\\ \vdots\\ -C_{n1}-C_{n2}-C_{n3}-\cdots-(s^2+C_{nn}) \end{bmatrix}, T^{'}(s)=\begin{bmatrix} T_1^{'}(s)\\ T_2^{'}(s)\\ T_3^{'}(s)\\ \vdots\\ T_n^{'}(s) \end{bmatrix}, T(s)=\begin{bmatrix} T_1(s)\\ T_2(s)\\ T_3(s)\\ \vdots\\ T_n(s) \end{bmatrix}. \tag{28}$$

By using the previous assumptions, we can then write system (27) as $A(s)T^{'}(s)=sT(s)$. Also, if $A(s)$ is invertible, we can then write it as follow:

$$T^{'}(s)=sA^{-1}(s)T(s). \tag{29}$$

System (29) can be then solved numerically by using a prepared MATLAB code with noting that $\phi_i(r)=\mathscr{L}^{-1}\{T_i(s)\}$, for all $i=1,2,\cdots,n$. This would give the solution $\phi_i(r)$ of system (24). This system is regarded as a homogeneous linear system with coefficient variables. The solution of system (29) is of the form:

$$T(s)=\phi(s)C, \tag{30}$$

where C is an n-dimensional vector consisting of arbitrary numbers. Note that $\phi(s)$ defined as follow:

$$\phi(s)=e^{\int_0^s \tau A(\tau)d\tau}. \tag{31}$$

Consequently, we get $T_i(s)=\mathscr{L}(\phi_i(r))$, for all $i=1,2,\cdots,n$. Also, we can find $\phi_i(r)=\mathscr{L}^{-1}(T_i(s)$, for all $i=1,2,\cdots,n$, which represents the desired solution of system (24).

3.1.3 Multi-group neutron diffusion system in slab reactor

The multi-group of neutrons diffusion system in slab reactor has the form

$$\begin{aligned}
&\phi_1^{''}(r)+C_{11}\phi_1(r)+C_{12}\phi_2(r)+C_{13}\phi_3(r)+\cdots+C_{1n}\phi_n(r)=0\\
&\phi_2^{''}(r)+C_{21}\phi_1(r)+C_{22}\phi_2(r)+C_{23}\phi_3(r)+\cdots+C_{2n}\phi_n(r)=0\\
&\phi_3^{''}(r)+C_{31}\phi_1(r)+C_{32}\phi_2(r)+C_{33}\phi_3(r)+\cdots+C_{3n}\phi_n(r)=0\\
&\vdots\\
&\phi_n^{''}(r)+C_{n1}\phi_1(r)+C_{n2}\phi_2(r)+C_{n3}\phi_3(r)+\cdots+C_{nn}\phi_n(r)=0,
\end{aligned} \tag{32}$$

with the following initial conditions:

$$\phi_i(0^+) = a_i,\ \phi_i^{'}(0^+) = b_i,\ \text{for all } i = 1, 2, \cdots, n. \tag{33}$$

By taking the Laplace transform of the both sides of the above system and by using the same manner of the spherical case, we get

$$\begin{aligned}
&s^2T_1(s) - a_1 s - b_1 + C_{11}T_1 s + C_{12}T_2 s + C_{13}T_3 s + \cdots + C_{1n}T_n s = 0,\\
&s^2T_2(s) - a_2 s - b_2 + C_{21}T_1 s + C_{22}T_2 s + C_{23}T_3 s + \cdots + C_{2n}T_n s = 0,\\
&s^2T_3(s) - a_3 s - b_3 + C_{31}T_1 s + C_{32}T_2 s + C_{33}T_3 s + \cdots + C_{3n}T_n s = 0,\\
&\vdots\\
&s^2T_n(s) - a_n s - b_n + C_{n1}T_1 s + C_{n2}T_2 s + C_{n3}T_3 s + \cdots + C_{nn}T_n s = 0.
\end{aligned} \tag{34}$$

In a similar manner to the previous subsections, the above system can be solved in frequency domain and then we can obtain the desired solution $\phi_i(r) = \mathscr{L}^{-1}(T_i(s))$ in the true domain by using MATLAB, for $i = 1, 2, \cdots, n$.

3.2 Fractional-order form of multi-group neutron diffusion system

In this subsection, we will introduce the fractional-order version of multi-group neutron diffusion equations (12). For this purpose, it should be first noted that $\nabla^2\phi_i(r)$ can be defined as follow:

$$\nabla^2\phi_i(r) = \phi_i^{''}(r) + \frac{a}{r}\phi_i^{'}(r), \tag{35}$$

for every $i = 1, \cdots, n$. Now, in view of (35), and by operating the Caputo differentiator on system (12), we obtain the following system:

$$\begin{aligned}
&D^{2\alpha}\phi_1(r) + \frac{a}{r}D^{\alpha}\phi_1(r) + C_{11}\phi_1(r) + C_{12}\phi_2(r) + C_{13}\phi_3(r) + \cdots + C_{1n}\phi_n(r) = 0,\\
&D^{2\alpha}\phi_2(r) + \frac{a}{r}D^{\alpha}\phi_2(r) + C_{21}\phi_1(r) + C_{22}\phi_2(r) + C_{23}\phi_3(r) + \cdots + C_{2n}\phi_n(r) = 0,\\
&D^{2\alpha}\phi_3(r) + \frac{a}{r}D^{\alpha}\phi_3(r) + C_{31}\phi_1(r) + C_{32}\phi_2(r) + C_{33}\phi_3(r) + \cdots + C_{3n}\phi_n(r) = 0,\\
&\vdots\\
&D^{2\alpha}\phi_n(r) + \frac{a}{r}D^{\alpha}\phi_n(r) + C_{n1}\phi_1(r) + C_{n2}\phi_2(r) + C_{n3}\phi_3(r) + \cdots + C_{nn}\phi_n(r) = 0.
\end{aligned} \tag{36}$$

Herein, the MFEM might be employed to find an approximate solution to the multi-group time-independent neutron diffusion system of equations (36) for three nuclear reactor essential geometries, namely spherical, cylindrical and slab reactors which will be studied based on the value of the parameter a, that it when $a = 2$, $a = 1$ and $a = 0$, respectively. But before dealing with this aim, we state and prove the next important result.

3.2.1 Reduction $n\alpha$-FDE to α-system of FDEs

In this part, we aim to reduce the FDE of order $n\alpha$ to a system of FDEs of order α, where $0 < \alpha \leq 1$. For this purpose, we provide the next lemma.

Lemma 3.1. *Any FDE of order $n\alpha$, $n \in \mathbb{Z}^+$ and $\alpha \in (0, 1]$, with functions possessing values in $\mathbb{R}$, can be converted into a system of FDEs of order α with values in $\mathbb{R}^{nd}$.*

Proof. To prove this result, we should first take the scalar case that takes place whenever $d = 1$ and then we will consider the remaining case that is hold when $d > 1$. For this reason, we should note that the general form of the FDE of order $n\alpha$ in its scaler case can be given by

$$D^{n\alpha}y(t) = G(t, y(t), D^{\alpha}y(t), D^{2\alpha}y(t), \cdots, D^{(n-1)\alpha}y(t)), \tag{37}$$

https://doi.org/10.54216/IJNS.240401

Received: September 25, 2023 Revised: February 19, 2024 Accepted: May 07, 2024

where G is a continuous function defined on the subset $I \times \mathbb{R} \times \mathbb{R} \times \cdots \times \mathbb{R}$ so that it takes values in $\mathbb{R}$ for a given intend I. Now, define the function

$$\mathbf{\Psi}(t, v_0, v_1, \cdots, v_{n-1}) = (v_1, v_2, \cdots, G(t, v_0, v_1, \cdots, v_{n-1})) \tag{38}$$

as a continuous function defined on $I \times \mathbb{R} \times \mathbb{R} \times \cdots \times \mathbb{R}$ as G, but it takes the values in $\mathbb{R}^n$. In this regard, we consider the following equation:

$$D^\alpha \mathbf{Y}(t) = \mathbf{\Psi}(t, \mathbf{Y}(t)), \text{ for } t \in I. \tag{39}$$

Now, we want to show that $x : I \to \mathbb{R}$ is a solution of equation (38) if and only if the function

$$\begin{aligned} \mathbf{X} :& I \to \mathbb{R}^n, \\ & t \to (x(t), D^\alpha x(t), D^{2\alpha} x(t), \cdots, D^{(n-1)\alpha} x(t)), \end{aligned} \tag{40}$$

is a solution of equation (39). To this end, we assume that x is a solution to equation (38) such that $\mathbf{X}$ is defined above. Then we have

$$D^\alpha \mathbf{X}(t) = \begin{pmatrix} D^\alpha x(t) \\ D^{2\alpha} x(t) \\ \vdots \\ D^{(n-1)\alpha} x(t) \\ D^{n\alpha} x(t) \end{pmatrix} = \begin{pmatrix} D^\alpha x(t) \\ D^{2\alpha} x(t) \\ \vdots \\ D^{(n-1)\alpha} x(t) \\ G(t, x(t), D^\alpha x(t), D^{2\alpha} x(t), \cdots, D^{(n-1)\alpha} x(t)) \end{pmatrix} = \mathbf{\Psi}(t, \mathbf{X}(t)). \tag{41}$$

Herein, the converse of the above discussion is similar. Now, for the case of $d > 1$, one can reread the above proof again, and substitute each occurrence of $\mathbb{R}$ by $\mathbb{R}^d$ to get the result. □

3.2.2 Fractional multi-group neutron diffusion system in spherical reactor

In this subsection, we will propose a fractional-order version of multi-group neutron diffusion system in a spherical reactor, and then obtain its numerical solution using Lemma 3.1 and the MFEM.[23] In fact, system (15) can be expressed in the fractional-order case as follows:

$$\begin{aligned} & rD^{2\alpha}\phi_1(r) + 2D^\alpha \phi_1(r) + rC_{11}\phi_1(r) + rC_{12}\phi_2(r) + rC_{13}\phi_3(r) + \cdots + rC_{1n}\phi_n(r) = 0, \\ & rD^{2\alpha}\phi_2(r) + 2D^\alpha \phi_2(r) + rC_{21}\phi_1(r) + rC_{22}\phi_2(r) + rC_{23}\phi_3(r) + \cdots + rC_{2n}\phi_n(r) = 0, \\ & rD^{2\alpha}\phi_3(r) + 2D^\alpha \phi_3(r) + rC_{31}\phi_1(r) + rC_{32}\phi_2(r) + rC_{33}\phi_3(r) + \cdots + rC_{3n}\phi_n(r) = 0, \\ & \vdots \\ & rD^{2\alpha}\phi_n(r) + 2D^\alpha \phi_n(r) + rC_{n1}\phi_1(r) + rC_{n2}\phi_2(r) + rC_{n3}\phi_3(r) + \cdots + rC_{nn}\phi_n(r) = 0. \end{aligned} \tag{42}$$

This system can be defined also by

$$\begin{aligned} & D^{2\alpha}\phi_1(r) = -\Big(\frac{2}{r} D^\alpha \phi_1(r) + C_{11}\phi_1(r) + C_{12}\phi_2(r) + C_{13}\phi_3(r) + \cdots + C_{1n}\phi_n(r)\Big), \\ & D^{2\alpha}\phi_2(r) = -\Big(\frac{2}{r} D^\alpha \phi_2(r) + C_{21}\phi_1(r) + C_{22}\phi_2(r) + C_{23}\phi_3(r) + \cdots + C_{2n}\phi_n(r)\Big), \\ & D^{2\alpha}\phi_3(r) = -\Big(\frac{2}{r} D^\alpha \phi_3(r) + C_{31}\phi_1(r) + C_{32}\phi_2(r) + C_{33}\phi_3(r) + \cdots + C_{3n}\phi_n(r)\Big), \\ & \vdots \\ & D^{2\alpha}\phi_n(r) = -\Big(\frac{2}{r} D^\alpha \phi_n(r) + C_{n1}\phi_1(r) + C_{n2}\phi_2(r) + C_{n3}\phi_3(r) + \cdots + C_{nn}\phi_n(r)\Big). \end{aligned} \tag{43}$$

Received: September 25, 2023 Revised: February 19, 2024 Accepted: May 07, 2024

Now, suppose that

$$
\begin{aligned}
&f_1(r,\phi_1,\phi_2,\phi_3,\cdots,\phi_n,D^{\alpha}\phi_1)\\
&\qquad = -\Big(\frac{2}{r}D^{\alpha}\phi_1(r)+C_{11}\phi_1(r)+C_{12}\phi_2(r)+C_{13}\phi_3(r)+\cdots+C_{1n}\phi_n(r)\Big),\\
&f_2(r,\phi_1,\phi_2,\phi_3,\cdots,\phi_n,D^{\alpha}\phi_2)\\
&\qquad = -\Big(\frac{2}{r}D^{\alpha}\phi_2(r)+C_{21}\phi_1(r)+C_{22}\phi_2(r)+C_{23}\phi_3(r)+\cdots+C_{2n}\phi_n(r)\Big),\\
&f_3(r,\phi_1,\phi_2,\phi_3,\cdots,\phi_n,D^{\alpha}\phi_3)\\
&\qquad = -\Big(\frac{2}{r}D^{\alpha}\phi_3(r)+C_{31}\phi_1(r)+C_{32}\phi_2(r)+C_{33}\phi_3(r)+\cdots+C_{3n}\phi_n(r)\Big),\\
&\qquad \vdots\\
&f_n(r,\phi_1,\phi_2,\phi_3,\cdots,\phi_n,D^{\alpha}\phi_n)\\
&\qquad = -\Big(\frac{2}{r}D^{\alpha}\phi_n(r)+C_{n1}\phi_1(r)+C_{n2}\phi_2(r)+C_{n3}\phi_3(r)+\cdots+C_{nn}\phi_n(r)\Big).
\end{aligned} \tag{44}
$$

Then, system (43) becomes

$$
\begin{aligned}
&D^{2\alpha}\phi_1(r)=f_1(r,\phi_1,\phi_2,\phi_3,\cdots,\phi_n,D^{\alpha}\phi_1),\\
&D^{2\alpha}\phi_2(r)=f_2(r,\phi_1,\phi_2,\phi_3,\cdots,\phi_n,D^{\alpha}\phi_2),\\
&D^{2\alpha}\phi_3(r)=f_3(r,\phi_1,\phi_2,\phi_3,\cdots,\phi_n,D^{\alpha}\phi_3),\\
&\vdots\\
&D^{2\alpha}\phi_n(r)=f_n(r,\phi_1,\phi_2,\phi_3,\cdots,\phi_n,D^{\alpha}\phi_n).
\end{aligned} \tag{45}
$$

If one assumes that $u_i = D^{\alpha}\phi_i(r)$, for all $i = 1, 2, \cdots, n$, we obtain

$$
\begin{aligned}
&D^{\alpha}\phi_1(r)=u_1=g_1(r,\phi_1,\phi_2,\phi_3,\cdots,\phi_n,u_1),\\
&D^{\alpha}u_1=D^{2\alpha}\phi_1(r)=f_1(r,\phi_1,\phi_2,\phi_3,\cdots,\phi_n,u_1),\\
&D^{\alpha}\phi_2(r)=u_2=g_2(r,\phi_1,\phi_2,\phi_3,\cdots,\phi_n,u_2),\\
&D^{\alpha}u_2=D^{2\alpha}\phi_2(r)=f_2(r,\phi_1,\phi_2,\phi_3,\cdots,\phi_n,u_2),\\
&D^{\alpha}\phi_3(r)=u_3=g_3(r,\phi_1,\phi_2,\phi_3,\cdots,\phi_n,u_3),\\
&D^{\alpha}u_3=D^{2\alpha}\phi_3(r)=f_3(r,\phi_1,\phi_2,\phi_3,\cdots,\phi_n,u_3),\\
&\vdots\\
&D^{\alpha}\phi_n(r)=u_n=g_n(r,\phi_1,\phi_2,\phi_3,\cdots,\phi_n,u_n),\\
&D^{\alpha}u_n=D^{2\alpha}\phi_n(r)=f_n(r,\phi_1,\phi_2,\phi_3,\cdots,\phi_n,u_n),
\end{aligned} \tag{46}
$$

with the following initial conditions:

$$\phi_i(0^+)=a_i,\ u_i(0^+)=b_i,\ \text{for all } i=1,2,\cdots,n. \tag{47}$$

It should be noted here that the above system represents a fractional-order system consisting of $2n$ fractional differential equations each of them is of order α. To solve this system, we shall use the MFEM. This can be carried out by first dividing the interval $I = [0^+, T]$ as $0^+ = t_0 < t_1 = t_0 + h < t_2 = t_0 + 2h < \cdots < t_n = t_0 + nh = T$ such that the mesh point are $t_i = t_0 + ih$, $i = 1, 2, \cdots, n$, with step size $h = T/n$. For simplicity, we denote $g_i(t, r, \phi_1, \phi_2, \cdots, \phi_n, u_i)$ and $f_i(t, r, \phi_1, \phi_2, \cdots, \phi_n, u_i)$ by g_i, f_i respectively, for all

https://doi.org/10.54216/IJNS.240401
Received: September 25, 2023 Revised: February 19, 2024 Accepted: May 07, 2024

$i = 1, 2, \cdots, n$. Now, based on the main formula of the MFEM, we can obtain the following states:

$$\begin{aligned}
&\phi_1(t_{i+1}) = \phi_1(t_i) + \frac{h^\alpha}{\Gamma(\alpha+1)} g_1\Big(t_i + \frac{h^\alpha}{2\Gamma(\alpha+1)}, \phi_1(t_i) + \frac{h^\alpha}{2\Gamma(\alpha+1)} g_1, \phi_2(t_i) + \frac{h^\alpha}{2\Gamma(\alpha+1)} g_2, \cdots,\\
&\phi_n(t_i) + \frac{h^\alpha}{2\Gamma(\alpha+1)} g_n, u_1(t_i) + \frac{h^\alpha}{2\Gamma(\alpha+1)} f_1\Big),\\
&u_1(t_{i+1}) = u_1(t_i) + \frac{h^\alpha}{\Gamma(\alpha+1)} f_1\Big(t_i + \frac{h^\alpha}{2\Gamma(\alpha+1)}, \phi_1(t_i) + \frac{h^\alpha}{2\Gamma(\alpha+1)} g_1, \phi_2(t_i) + \frac{h^\alpha}{2\Gamma(\alpha+1)} g_2, \cdots,\\
&\phi_n(t_i) + \frac{h^\alpha}{2\Gamma(\alpha+1)} g_n, u_1(t_i) + \frac{h^\alpha}{2\Gamma(\alpha+1)} f_1\Big),\\
&\phi_2(t_{i+1}) = \phi_2(t_i) + \frac{h^\alpha}{\Gamma(\alpha+1)} g_2\Big(t_i + \frac{h^\alpha}{2\Gamma(\alpha+1)}, \phi_1(t_i) + \frac{h^\alpha}{2\Gamma(\alpha+1)} g_1, \phi_2(t_i) + \frac{h^\alpha}{2\Gamma(\alpha+1)} g_2, \cdots,\\
&\phi_n(t_i) + \frac{h^\alpha}{2\Gamma(\alpha+1)} g_n, u_2(t_i) + \frac{h^\alpha}{2\Gamma(\alpha+1)} f_2\Big),\\
&u_2(t_{i+1}) = u_2(t_i) + \frac{h^\alpha}{\Gamma(\alpha+1)} f_2\Big(t_i + \frac{h^\alpha}{2\Gamma(\alpha+1)}, \phi_1(t_i) + \frac{h^\alpha}{2\Gamma(\alpha+1)} g_1, \phi_2(t_i) + \frac{h^\alpha}{2\Gamma(\alpha+1)} g_2, \cdots,\\
&\phi_n(t_i) + \frac{h^\alpha}{2\Gamma(\alpha+1)} g_n, u_2(t_i) + \frac{h^\alpha}{2\Gamma(\alpha+1)} f_2\Big),\\
&\phi_3(t_{i+1}) = \phi_3(t_i) + \frac{h^\alpha}{\Gamma(\alpha+1)} g_3\Big(t_i + \frac{h^\alpha}{2\Gamma(\alpha+1)}, \phi_1(t_i) + \frac{h^\alpha}{2\Gamma(\alpha+1)} g_1, \phi_2(t_i) + \frac{h^\alpha}{2\Gamma(\alpha+1)} g_2, \cdots,\\
&\phi_n(t_i) + \frac{h^\alpha}{2\Gamma(\alpha+1)} g_n, u_3(t_i) + \frac{h^\alpha}{2\Gamma(\alpha+1)} f_3\Big),\\
&u_3(t_{i+1}) = u_3(t_i) + \frac{h^\alpha}{\Gamma(\alpha+1)} f_3\Big(t_i + \frac{h^\alpha}{2\Gamma(\alpha+1)}, \phi_1(t_i) + \frac{h^\alpha}{2\Gamma(\alpha+1)} g_1, \phi_2(t_i) + \frac{h^\alpha}{2\Gamma(\alpha+1)} g_2, \cdots,\\
&\phi_n(t_i) + \frac{h^\alpha}{2\Gamma(\alpha+1)} g_n, u_3(t_i) + \frac{h^\alpha}{2\Gamma(\alpha+1)} f_3\Big),\\
&\vdots\\
&\phi_n(t_{i+1}) = \phi_n(t_i) + \frac{h^\alpha}{\Gamma(\alpha+1)} g_n\Big(t_i + \frac{h^\alpha}{2\Gamma(\alpha+1)}, \phi_1(t_i) + \frac{h^\alpha}{2\Gamma(\alpha+1)} g_1, \phi_2(t_i) + \frac{h^\alpha}{2\Gamma(\alpha+1)} g_2, \cdots,\\
&\phi_n(t_i) + \frac{h^\alpha}{2\Gamma(\alpha+1)} g_n, u_n(t_i) + \frac{h^\alpha}{2\Gamma(\alpha+1)} f_n\Big),\\
&u_n(t_{i+1}) = u_n(t_i) + \frac{h^\alpha}{\Gamma(\alpha+1)} f_2\Big(t_i + \frac{h^\alpha}{2\Gamma(\alpha+1)}, \phi_1(t_i) + \frac{h^\alpha}{2\Gamma(\alpha+1)} g_1, \phi_2(t_i) + \frac{h^\alpha}{2\Gamma(\alpha+1)} g_2, \cdots,\\
&\phi_n(t_i) + \frac{h^\alpha}{2\Gamma(\alpha+1)} g_n, u_n(t_i) + \frac{h^\alpha}{2\Gamma(\alpha+1)} f_n\Big),
\end{aligned} \tag{48}$$

for $i = 1, 2, \cdots, n-1$. The previous system (48) represents an approximate solution of system (46), and hence $(\phi_1(t), \phi_2(t), \phi_3(t), \cdots, \phi_n(t))$ is then the defined solution of system (42).

3.2.3 Fractional multi-group neutron diffusion system in cylindrical reactor

In this part, we will express the fractional multi-group neutron diffusion system in cylindrical reactor, then we obtain its numerical solution by using reduction lemma (Lemma 3.1) and MFEM. In fact, system (24) can be

https://doi.org/10.54216/IJNS.240401
Received: September 25, 2023 Revised: February 19, 2024 Accepted: May 07, 2024

reexpressed in light of the cylindrical reactor in its fractional-order case as follow:

$$\begin{aligned}
&rD^{2\alpha}\phi_1(r) + D^{\alpha}\phi_1(r) + r\Big(C_{11}\phi_1(r) + C_{12}\phi_2(r) + C_{13}\phi_3(r) + \cdots + C_{1n}\phi_n(r)\Big) = 0,\\
&rD^{2\alpha}\phi_2(r) + D^{\alpha}\phi_2(r) + r\Big(C_{21}\phi_1(r) + C_{22}\phi_2(r) + C_{23}\phi_3(r) + \cdots + C_{2n}\phi_n(r)\Big) = 0,\\
&rD^{2\alpha}\phi_3(r) + D^{\alpha}\phi_3(r) + r\Big(C_{31}\phi_1(r) + C_{32}\phi_2(r) + C_{33}\phi_3(r) + \cdots + C_{3n}\phi_n(r)\Big) = 0,\\
&\vdots\\
&rD^{2\alpha}\phi_n(r) + D^{\alpha}\phi_n(r) + r\Big(C_{n1}\phi_1(r) + C_{n2}\phi_2(r) + C_{n3}\phi_3(r) + \cdots + C_{nn}\phi_n(r)\Big) = 0.
\end{aligned} \tag{49}$$

The same solution for system (48) can be regarded as an approximate solution of the previous system (49), but here the f_i should be assumed as follows:

$$\begin{aligned}
&f_1(r,\phi_1,\phi_2,\phi_3,\cdots,\phi_n,D^{\alpha}\phi_1)\\
&\qquad = -\Big(\frac{1}{r}D^{\alpha}\phi_1(r) + C_{11}\phi_1(r) + C_{12}\phi_2(r) + C_{13}\phi_3(r) + \cdots + C_{1n}\phi_n(r)\Big),\\
&f_2(r,\phi_1,\phi_2,\phi_3,\cdots,\phi_n,D^{\alpha}\phi_2)\\
&\qquad = -\Big(\frac{1}{r}D^{\alpha}\phi_2(r) + C_{21}\phi_1(r) + C_{22}\phi_2(r) + C_{23}\phi_3(r) + \cdots + C_{2n}\phi_n(r)\Big),\\
&f_3(r,\phi_1,\phi_2,\phi_3,\cdots,\phi_n,D^{\alpha}\phi_3)\\
&\qquad = -\Big(\frac{1}{r}D^{\alpha}\phi_3(r) + C_{31}\phi_1(r) + C_{32}\phi_2(r) + C_{33}\phi_3(r) + \cdots + C_{3n}\phi_n(r)\Big),\\
&\qquad\vdots\\
&f_n(r,\phi_1,\phi_2,\phi_3,\cdots,\phi_n,D^{\alpha}\phi_n)\\
&\qquad = -\Big(\frac{1}{r}D^{\alpha}\phi_n(r) + C_{n1}\phi_1(r) + C_{n2}\phi_2(r) + C_{n3}\phi_3(r) + \cdots + C_{nn}\phi_n(r)\Big).
\end{aligned} \tag{50}$$

3.2.4 Fractional multi-group neutron diffusion system in slab reactor

In this subsection, we aim to propose a fractional-order version of the multi-group neutron diffusion system in the slab reactor, and then obtain its numerical solution using Lemma 3.1 and MFEM. In fact, system (32) can be fractionalized in view of the slab reactor as follows:

$$\begin{aligned}
&D^{2\alpha}\phi_1(r) + C_{11}\phi_1(r) + C_{12}\phi_2(r) + C_{13}\phi_3(r) + \cdots + C_{1n}\phi_n(r) = 0,\\
&D^{2\alpha}\phi_2(r) + C_{21}\phi_1(r) + C_{22}\phi_2(r) + C_{23}\phi_3(r) + \cdots + C_{2n}\phi_n(r) = 0,\\
&D^{2\alpha}\phi_3(r) + C_{31}\phi_1(r) + C_{32}\phi_2(r) + C_{33}\phi_3(r) + \cdots + C_{3n}\phi_n(r) = 0,\\
&\vdots\\
&D^{2\alpha}\phi_n(r) + C_{n1}\phi_1(r) + C_{n2}\phi_2(r) + C_{n3}\phi_3(r) + \cdots + C_{nn}\phi_n(r) = 0.
\end{aligned} \tag{51}$$

https://doi.org/10.54216/IJNS.240401

Received: September 25, 2023 Revised: February 19, 2024 Accepted: May 07, 2024

The same solution for system (48) can also be regarded as an approximate solution of the previous system (51), but here the f_i should be assumed as follows:

$$\begin{aligned}
&f_1(r,\phi_1,\phi_2,\phi_3,\cdots,\phi_n) = -\Big(C_{11}\phi_1(r)+C_{12}\phi_2(r)+C_{13}\phi_3(r)+\cdots+C_{1n}\phi_n(r)\Big),\\
&f_2(r,\phi_1,\phi_2,\phi_3,\cdots,\phi_n) = -\Big(C_{21}\phi_1(r)+C_{22}\phi_2(r)+C_{23}\phi_3(r)+\cdots+C_{2n}\phi_n(r)\Big),\\
&f_3(r,\phi_1,\phi_2,\phi_3,\cdots,\phi_n) = -\Big(C_{31}\phi_1(r)+C_{32}\phi_2(r)+C_{33}\phi_3(r)+\cdots+C_{3n}\phi_n(r)\Big),\\
&\vdots\\
&f_n(r,\phi_1,\phi_2,\phi_3,\cdots,\phi_n) = -\Big(C_{n1}\phi_1(r)+C_{n2}\phi_2(r)+C_{n3}\phi_3(r)+\cdots+C_{nn}\phi_n(r)\Big).
\end{aligned} \tag{52}$$

4 Illustrative numerical simulations

Investigating the flux behavior in the reactor is important for reactor performance and safety. Typically, that flux, indicating the number of neutrons flowing, has its maximum value at the center of the reactor and decreases at the surface. Traditionally, it's thought that flux diminishes at the reactor surface based on the zero-flux boundary condition that is commonly used for simulating reactor behavior.

This section numerically analyzes all energy flux behaviors in nuclear reactors and their effects on reactor simulation outcomes. The study evaluates the influence on simulation accuracy and reliability. This research contributes to nuclear system modeling and emphasizes the significance of suitable boundary conditions in reactor simulations. In particular, we will introduce the three cases of multi-group neutron diffusion systems related to spherical reactor, cylindrical reactor, and slap reactor. For this purpose, we list in the following Table (1) obtained from[6] is correspondingly used. According to the data given in Table 1, the values of C_{ij} can be determined as shown in Table (2). In the same regard, we consider the following initial conditions to be applicable:

$$\phi_1(0.0002) = 1,\ \phi_2(0.0002) = 4.21,\ \phi_3(0.0002) = 2.764,\ \phi_4(0.0002) = 3.118,$$

and

$$D^\alpha\phi_1(0.0002) = 0,\ D^\alpha\phi_2(0.0002) = 0,\ D^\alpha\phi_3(0.0002) = 0,\ D^\alpha\phi_4(0.0002) = 0.$$

The following subsections show numerical results for each reactor geometry.

4.1 Spherical reactor

The fractional multi-group neutron diffusion system associated with spherical reactor is addressed in this subsection. With the use of the scheme discussed in Subsection 3.1.1, the classical system (15) is numerically solved by LTM, and then compared with the numerical solution $(\phi_1(r),\phi_2(r),\phi_3(r),\phi_4(r))$ of system (42) obtained by MFEM when $\alpha = 1$. The overall comparison between these two numerical solutions is depicted in Figure 1.

In Figures 2, 3, 4, and 5, we present, respectively, several numerical comparisons for $\phi_1(r)$, $\phi_2(r)$, $\phi_3(r)$, and $\phi_4(r)$ between MFEM's solutions according to different values of α.

For more illustration, in Figures 6, 7, 8 and 9, we plot respectively several numerical comparisons for $\phi_1(r)$, $\phi_2(r)$, $\phi_3(r)$, and $\phi_4(r)$ between LTM's and MFEM's solutions when $\alpha = 0.950, 0.975, 1$.

https://doi.org/10.54216/IJNS.240401

Received: September 25, 2023 Revised: February 19, 2024 Accepted: May 07, 2024

Table 1: Group Data

	Group 1 (1.35 Mev- 10 Mev)	
$\nu_1 \sum_{f_1} = 0.0096cm^{-1}$ $\sum_{S13} = 0.00cm^{-1}$	$\sum_a = 0.0049cm^{-1}$ $\sum_{S14} = 0.00cm^{-1}$ $\chi_1 = 0.575$	$\sum_{S12} = 0.0831cm^{-1}$ $D_1 = 2.162cm$
	Group 2 (9.1 kev - 1.35 Mev)	
$\nu_2 \sum_{f_2} = 0.0012cm^{-1}$ $\sum_{S22} = 0.00585cm^{-1}$	$\sum_{a2} = 0.0028cm^{-1}$ $\sum_{S23} = 0.00cm^{-1}$ $\chi_2 = 0.425$	$\sum_{S21} = 0.00cm^{-1}$ $D_2 = 1.087cm$
	Group 3 (0.4 ev - 9.1 kev)	
$\nu_3 \sum_{f_3} = 0.00177cm^{-1}$ $\sum_{S32} = 0.00cm^{-1}$	$\sum_{a3} = 0.00305cm^{-1}$ $\sum_{S33} = 0.0651cm^{-1}$ $\chi_3 = 0.0$	$\sum_{S31} = 0.00cm^{-1}$ $D_3 = 0.632cm$
	Group 4 (0.0 ev - 0.4 ev)	
$\nu_4 \sum_{f_4} = 0.1851cm^{-1}$ $\sum_{S42} = 0.00cm^{-1}$	$\sum_{a4} = 0.1210cm^{-1}$ $\sum_{S43} = 0.00cm^{-1}$ $\chi_4 = 0.0$	$\sum_{S41} = 0.00cm^{-1}$ $D_4 = 0.354cm$

Table 2: The values of the coefficients C_{ij} where $i, j = 1, 2, 3, 4$ are calculated from Equation (13)

C_{ij}	$i = 1$	$i = 2$	$i = 3$	$i = 4$
$j = 1$	-0.038150	0.080202	0.092563	0.183898
$j = 2$	0.000319	-0.055925	0.092563	0.183898
$j = 3$	0.004707	0.083370	-0.151266	0.183898
$j = 4$	0.049229	0.148820	0.092563	-0.341808

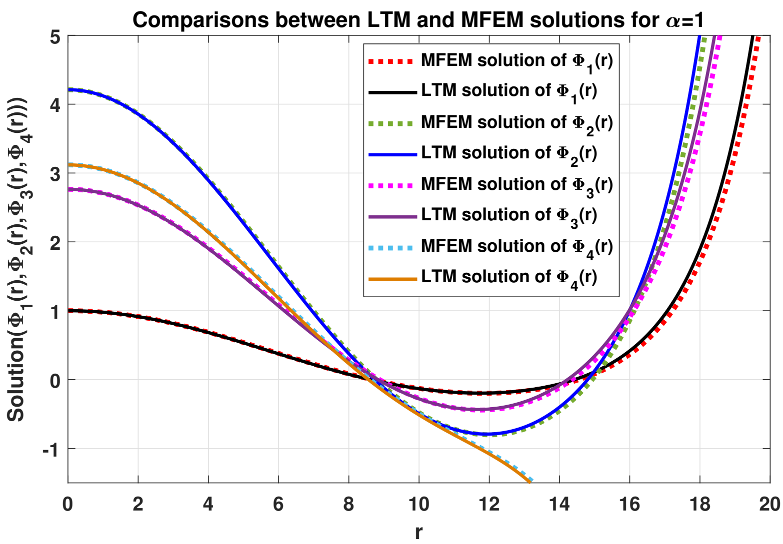

Figure 1: LTM's solution vs. MFEM's solution for multi-group neutron diffusion system in spherical reactor for $\alpha = 1$.

https://doi.org/10.54216/IJNS.240401

Received: September 25, 2023 Revised: February 19, 2024 Accepted: May 07, 2024

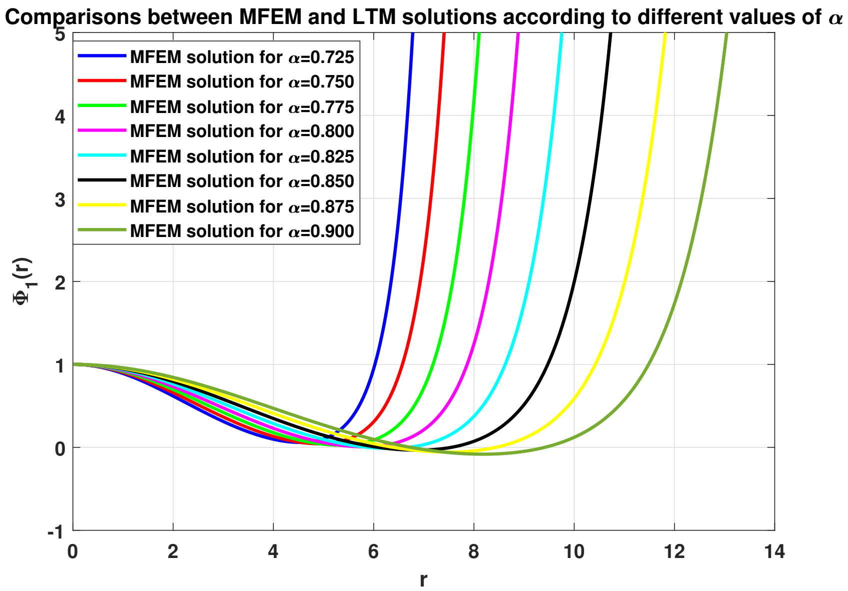

Figure 2: MFEM's solutions of $\phi_1(r)$ in spherical reactor for different values of α.

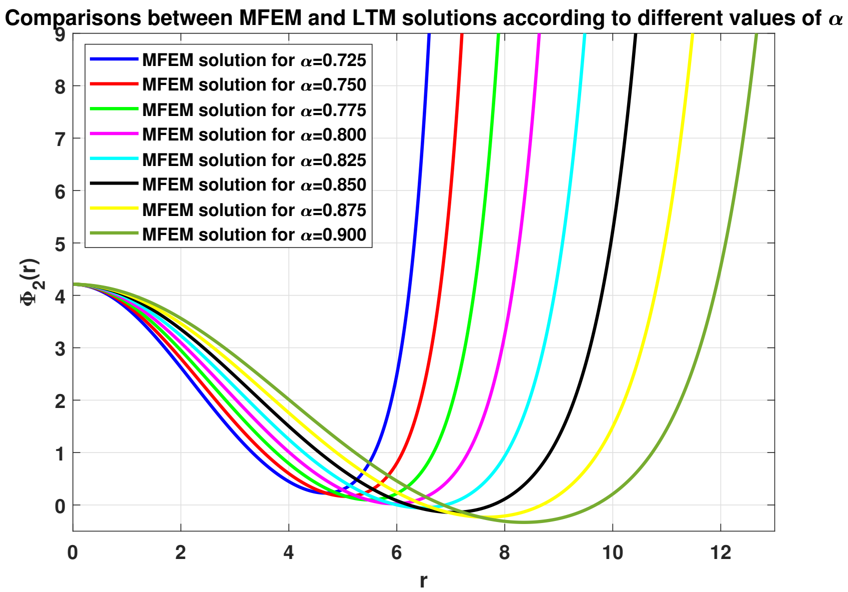

Figure 3: MFEM's solutions of $\phi_2(r)$ in spherical reactor for different values of α.

https://doi.org/10.54216/IJNS.240401
Received: September 25, 2023 Revised: February 19, 2024 Accepted: May 07, 2024

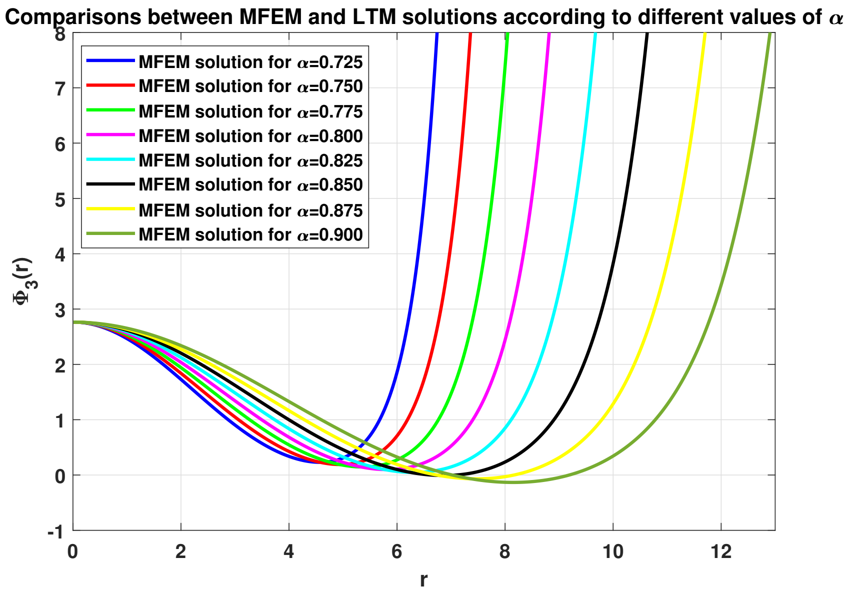

Figure 4: MFEM's solutions of $\phi_3(r)$ in spherical reactor for different values of α.

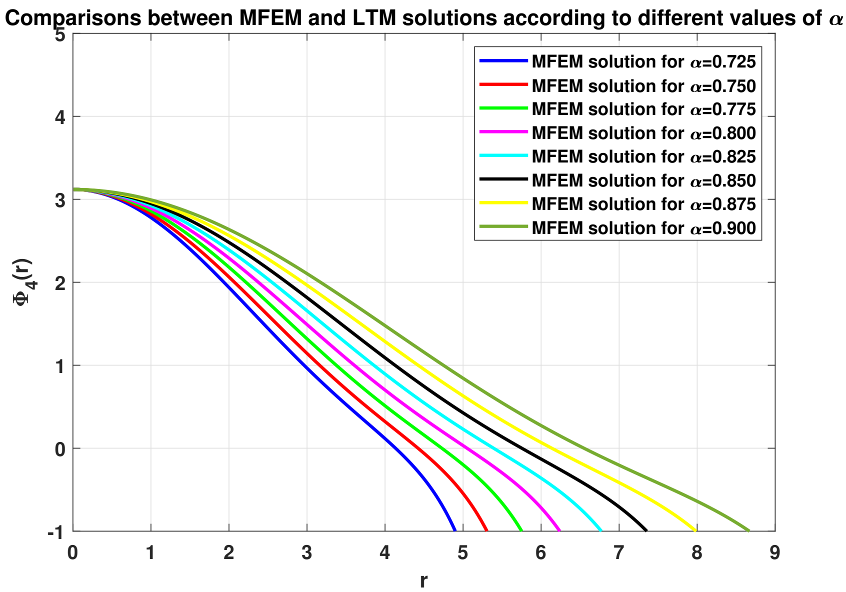

Figure 5: MFEM's solutions of $\phi_4(r)$ in spherical reactor for different values of α.

https://doi.org/10.54216/IJNS.240401

Received: September 25, 2023 Revised: February 19, 2024 Accepted: May 07, 2024

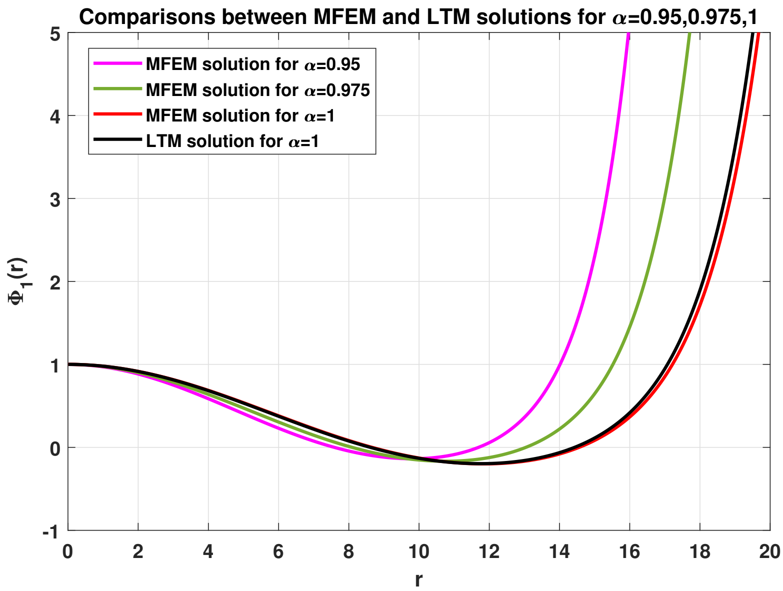

Figure 6: LTM's and MFEM's solutions of $\phi_1(r)$ in spherical reactor for $\alpha = 0.95, 0.975, 1$.

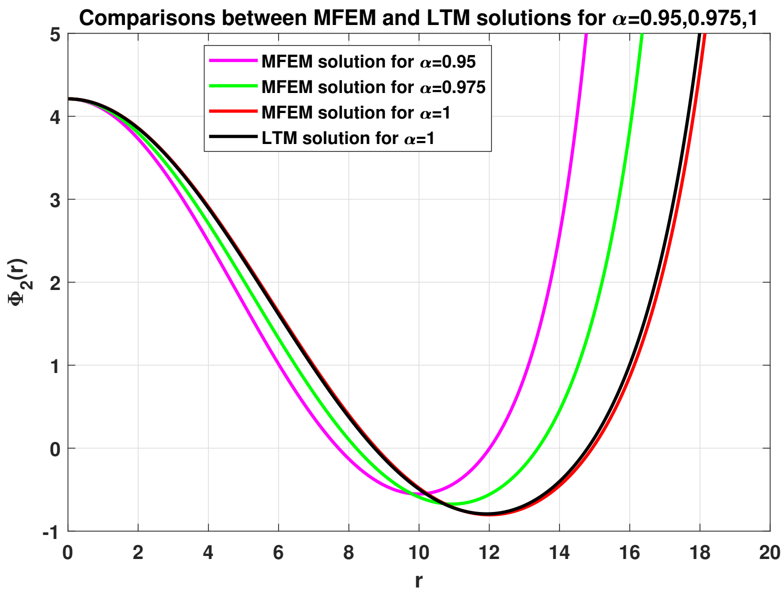

Figure 7: LTM's and MFEM's solutions of $\phi_2(r)$ in spherical reactor for $\alpha = 0.95, 0.975, 1$.

https://doi.org/10.54216/IJNS.240401
Received: September 25, 2023 Revised: February 19, 2024 Accepted: May 07, 2024

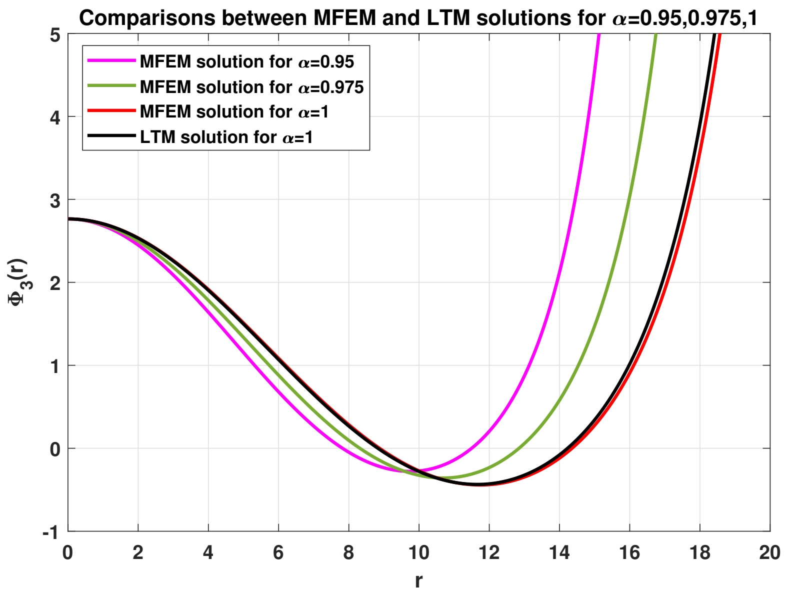

Figure 8: LTM's and MFEM's solutions of $\phi_3(r)$ in spherical reactor for $\alpha = 0.95, 0.975, 1$.

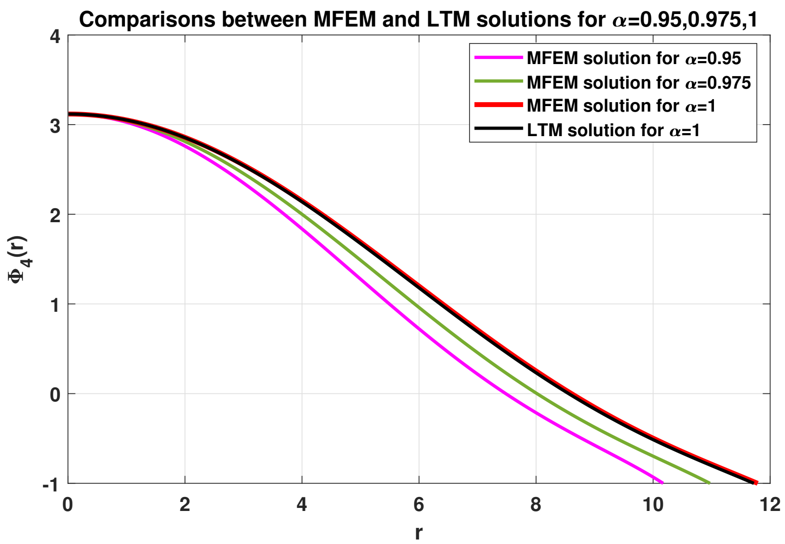

Figure 9: LTM's and MFEM's solutions of $\phi_4(r)$ in spherical reactor for $\alpha = 0.95, 0.975, 1$.

https://doi.org/10.54216/IJNS.240401
Received: September 25, 2023 Revised: February 19, 2024 Accepted: May 07, 2024

4.2 Cylindrical reactor

This subsection discusses the fractional multi-group neutron diffusion system connected to the spherical reactor. The classical system (24) is numerically solved by LTM using the scheme described in Subsection 3.1.1. The numerical solution $(\phi_1(r), \phi_2(r), \phi_3(r), \phi_4(r))$ of system (49) produced by MFEM when $\alpha = 1$ is then compared with it. Figure 10 shows the general comparison of these two numerical solutions.

In Figures 11, 12, 13, and 14, we present, respectively, several numerical comparisons for $\phi_1(r)$, $\phi_2(r)$, $\phi_3(r)$, and $\phi_4(r)$ between MFEM's solutions according to different values of α.

For more illustration, in Figures 15, 16, 17 and 18, we plot respectively several numerical comparisons for $\phi_1(r)$, $\phi_2(r)$, $\phi_3(r)$, and $\phi_4(r)$ between LTM's and MFEM's solutions when $\alpha = 0.950, 0.975, 1$.

4.3 Slab reactor

This subsection discusses the spherical reactor's fractional multi-group neutron diffusion system. The numerical solution $(\phi_1(r), \phi_2(r), \phi_3(r), \phi_4(r))$ of system (51) produced by MFEM when $\alpha = 1$ is compared with the numerical solution of the classical system (32) using the scheme described in Subsection 3.1.1. However, Figure 19 presents an overall comparison of these two numerical solutions.

In Figures 20, 21, 22, and 23, we present, respectively, several numerical comparisons for $\phi_1(r)$, $\phi_2(r)$, $\phi_3(r)$, and $\phi_4(r)$ between MFEM's solutions according to different values of α.

For more illustration, in Figures 24, 25, 26 and 27, we plot respectively several numerical comparisons for $\phi_1(r)$, $\phi_2(r)$, $\phi_3(r)$, and $\phi_4(r)$ between LTM's and MFEM's solutions when $\alpha = 0.950, 0.975, 1$.

5 Discussion

In view of all previous discussed cases, we can state the following observations:

- The numerical solution of the integer-order multi-group neutron diffusion system generated by the LTM is coincided with the numerical solution of the fractional-order multi-group neutron diffusion system generated by the MFEM when $\alpha = 1$ as one can see in Figures 1, 6, 7, 8, 9, 10, 15, 16, 17, 18, 19, 24, 25, 26, and 27.
- The influence of the fractional-order values on the multi-group neutron diffusion system of equations lies in capturing memory effects, non-local interactions, and anomalous behaviors that are not adequately described by classical integer-order models. This could apply to subdiffusion or superdiffusion in the context of neutron diffusion, where the neutron flux behaves differently than in the traditional diffusion model, see Figures 2, 3, 4, 5, 11, 12, 13, 14, 20, 21, 22, and 23.
- The stability of the two numerical schemes used to solve all cases of the integer- or fractional multi-group neutron diffusion system has been fulfilled whenever all fluxes converge at the boundary of the nuclear reactor. This what is known physically as the zero-flux boundary condition, and it can clearly be seen in all provided figures. For instance, one might observe that all fluxes depicted in Figure 1 go to zero at $r \approx 8.6$ in the spherical reactor, whereas all fluxes go to zero at $r \approx 7$ in the cylindrical reactor, as shown in Figure 10, and also they go to zero at $r \approx 4.3$ in the slab reactor as shown in Figure 19.
- In integer/fractional multi-group neutron diffusion system, the steady state is the state in which the distribution of neutron flux within the reactor remains constant across time. Stated differently, all characteristics pertaining to neutrons, including neutron flux, power distribution, and other pertinent quantities, become independent of time. Because it reflects the ideal operational state in which the reactor is stable and running at a constant power level, this steady-state condition is essential to understanding reactor operation and design. In the steady state, the time derivative of the neutron flux becomes zero, i.e.,
$$\frac{\partial \phi_i(r)}{\partial t} = \frac{\partial^\alpha \phi_i(r)}{\partial^\alpha t} = 0.$$
As a result, the neutron flux $\phi_i(r)$ becomes independent of time, for all $i = 1, 2, \cdots, n$.

https://doi.org/10.54216/IJNS.240401

Received: September 25, 2023 Revised: February 19, 2024 Accepted: May 07, 2024

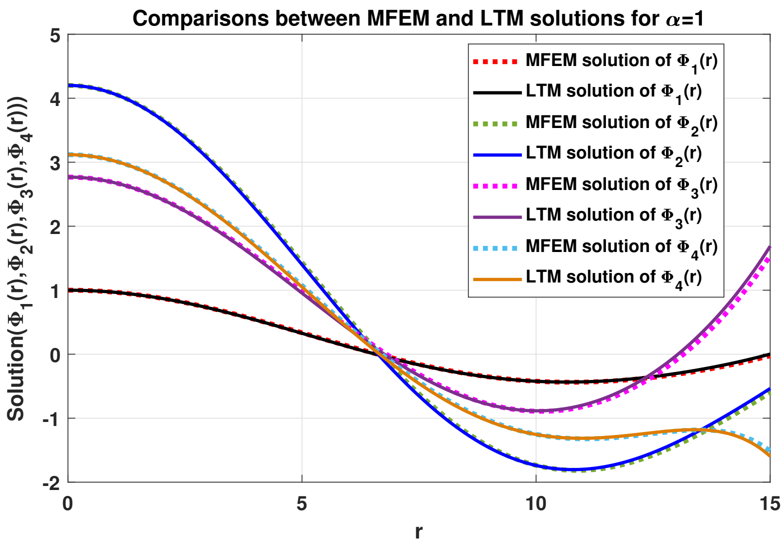

Figure 10: LTM's solution vs. MFEM's solution for multi-group neutron diffusion system in cylindrical reactor for $\alpha = 1$.

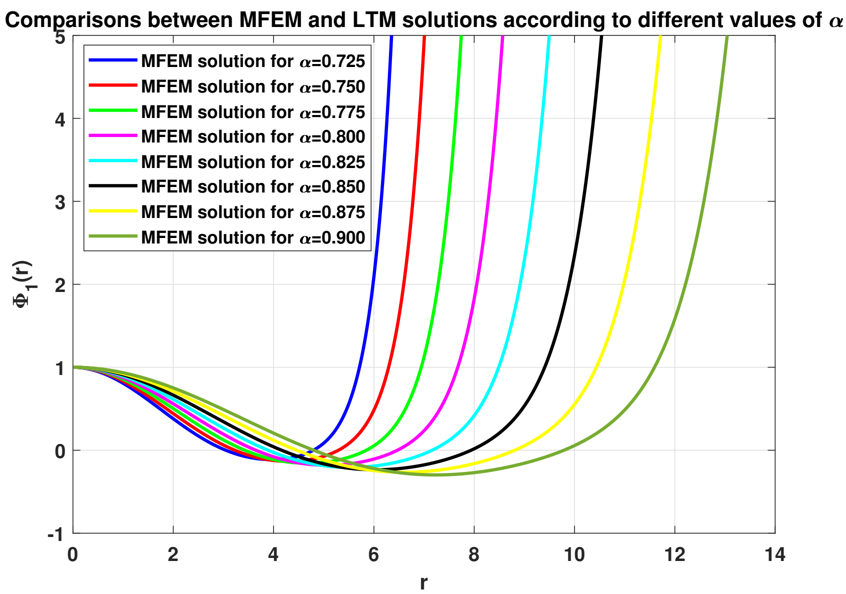

Figure 11: MFEM's solutions of $\phi_1(r)$ in cylindrical reactor for different values of α.

Received: September 25, 2023 Revised: February 19, 2024 Accepted: May 07, 2024

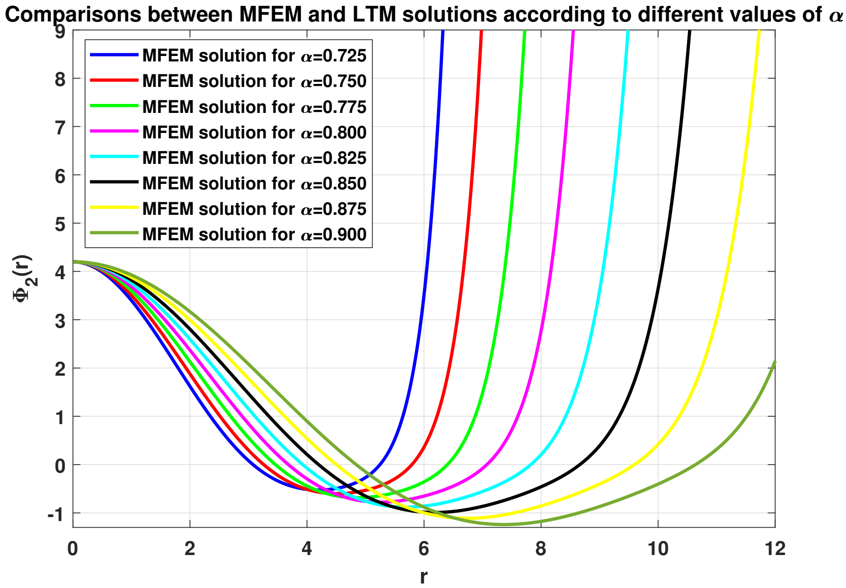

Figure 12: MFEM's solutions of $\phi_2(r)$ in cylindrical reactor for different values of α.

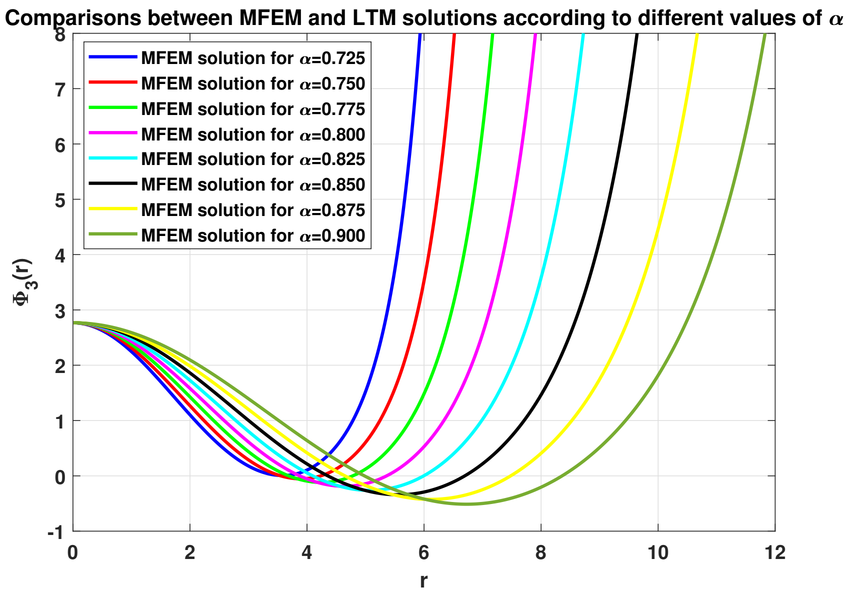

Figure 13: MFEM's solutions of $\phi_3(r)$ in cylindrical reactor for different values of α.

https://doi.org/10.54216/IJNS.240401
Received: September 25, 2023 Revised: February 19, 2024 Accepted: May 07, 2024

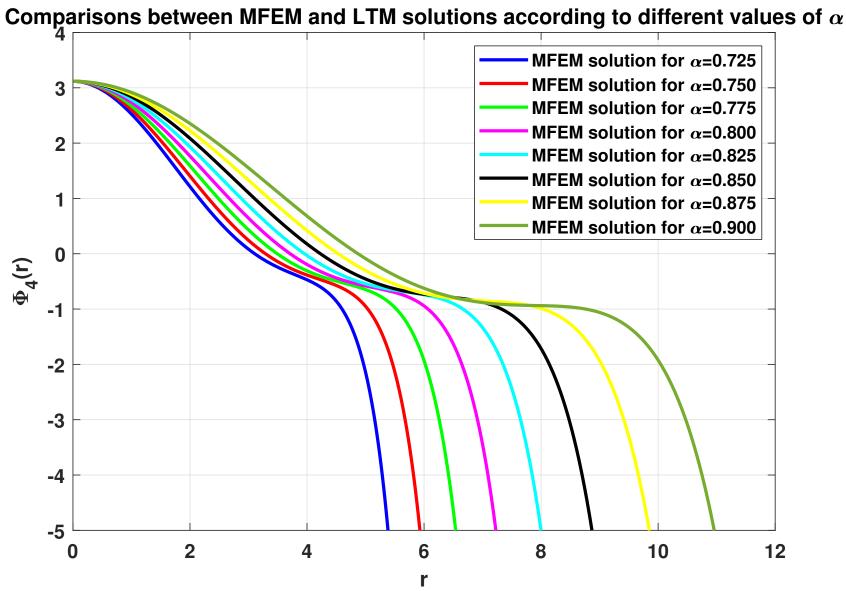

Figure 14: MFEM's solutions of $\phi_4(r)$ in cylindrical reactor for different values of α.

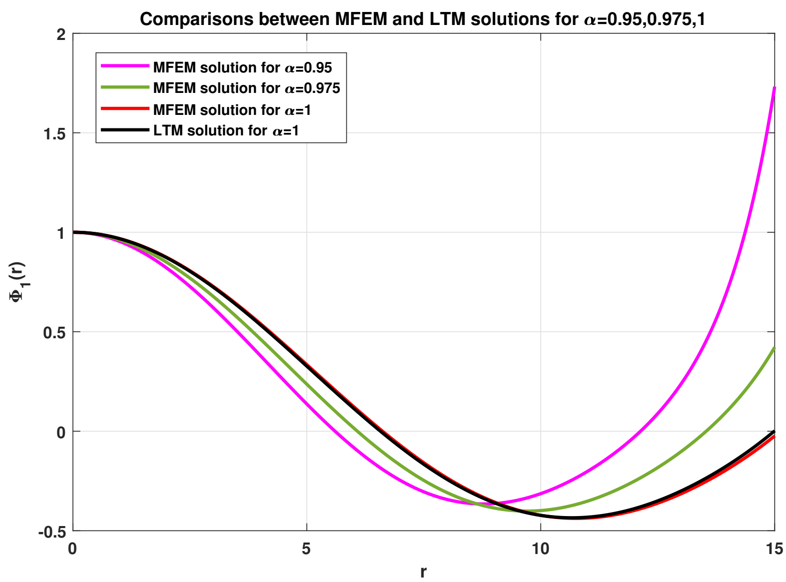

Figure 15: LTM's and MFEM's solutions of $\phi_1(r)$ in cylindrical reactor for $\alpha = 0.95, 0.975, 1$.

https://doi.org/10.54216/IJNS.240401

Received: September 25, 2023 Revised: February 19, 2024 Accepted: May 07, 2024

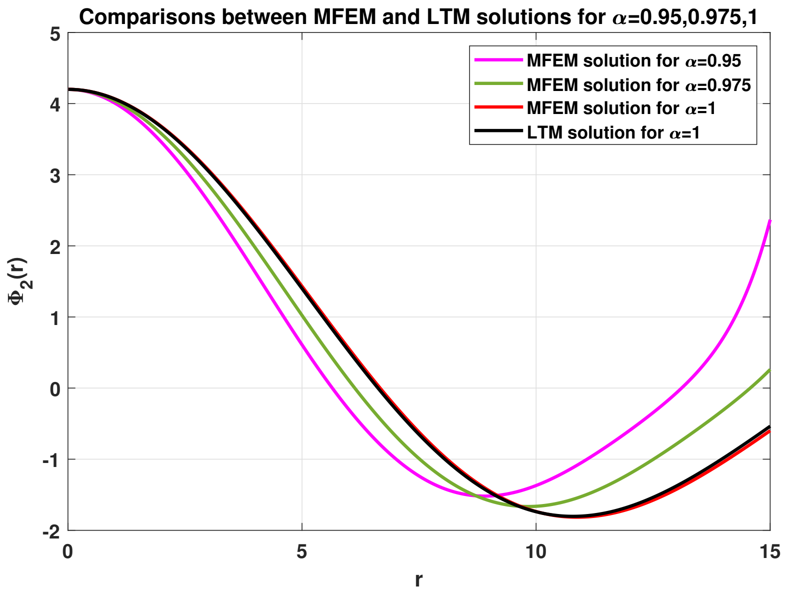

Figure 16: LTM's and MFEM's solutions of $\phi_2(r)$ in cylindrical reactor for $\alpha = 0.95, 0.975, 1$.

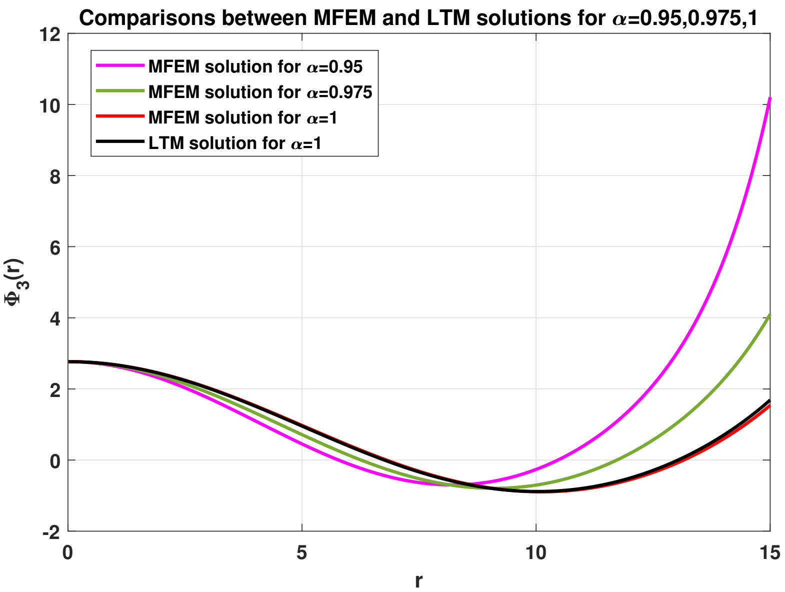

Figure 17: LTM's and MFEM's solutions of $\phi_3(r)$ in cylindrical reactor for $\alpha = 0.95, 0.975, 1$.

https://doi.org/10.54216/IJNS.240401
Received: September 25, 2023 Revised: February 19, 2024 Accepted: May 07, 2024

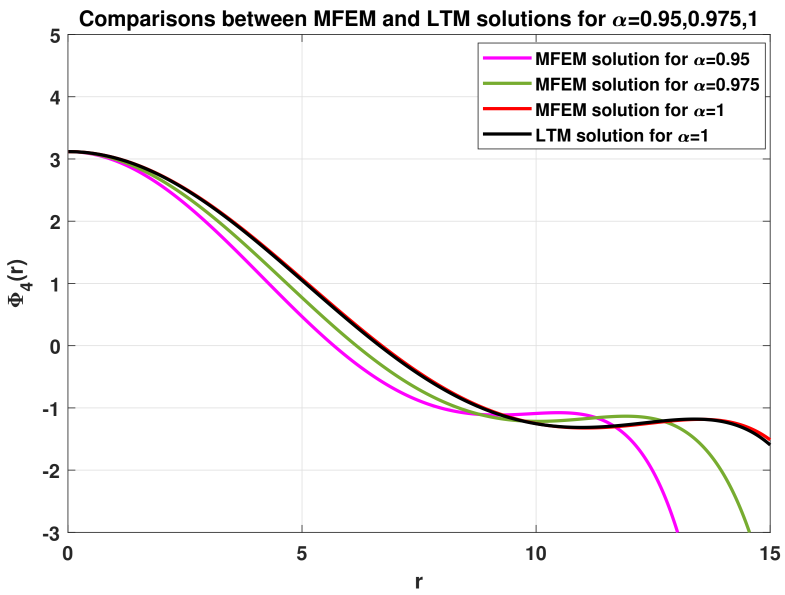

Figure 18: LTM's and MFEM's solutions of $\phi_4(r)$ in cylindrical reactor for $\alpha = 0.95, 0.975, 1$.

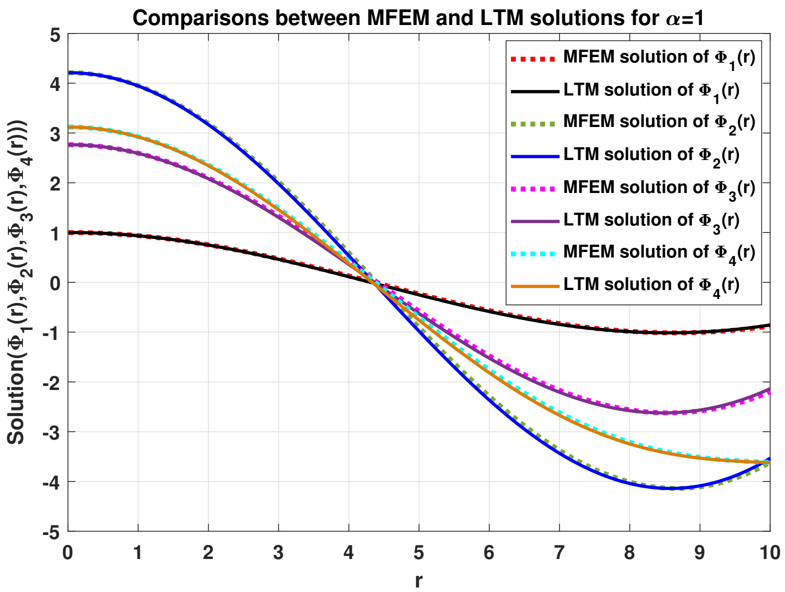

Figure 19: LTM's solution vs. MFEM's solution for multi-group neutron diffusion system in slab reactor for $\alpha = 1$.

https://doi.org/10.54216/IJNS.240401

Received: September 25, 2023 Revised: February 19, 2024 Accepted: May 07, 2024

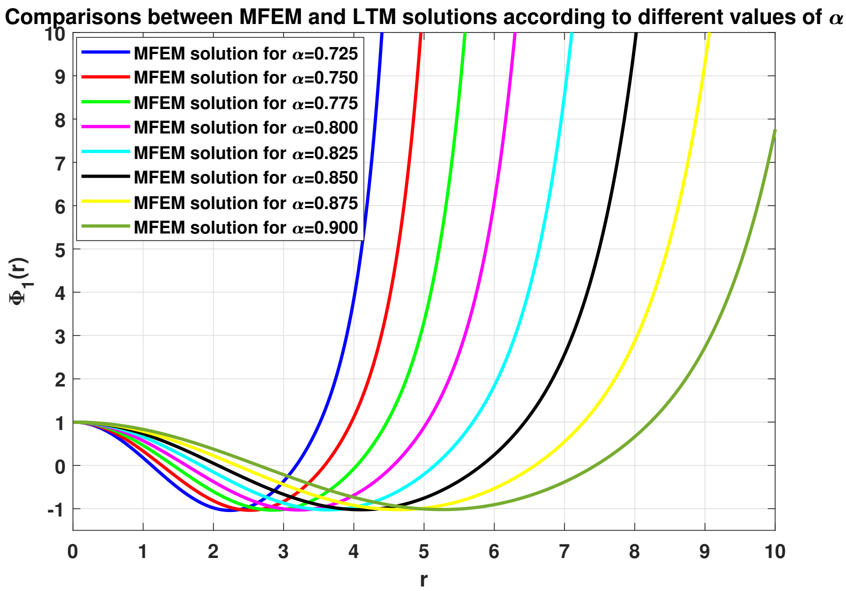

Figure 20: MFEM's solutions of $\phi_1(r)$ in slab reactor for different values of α.

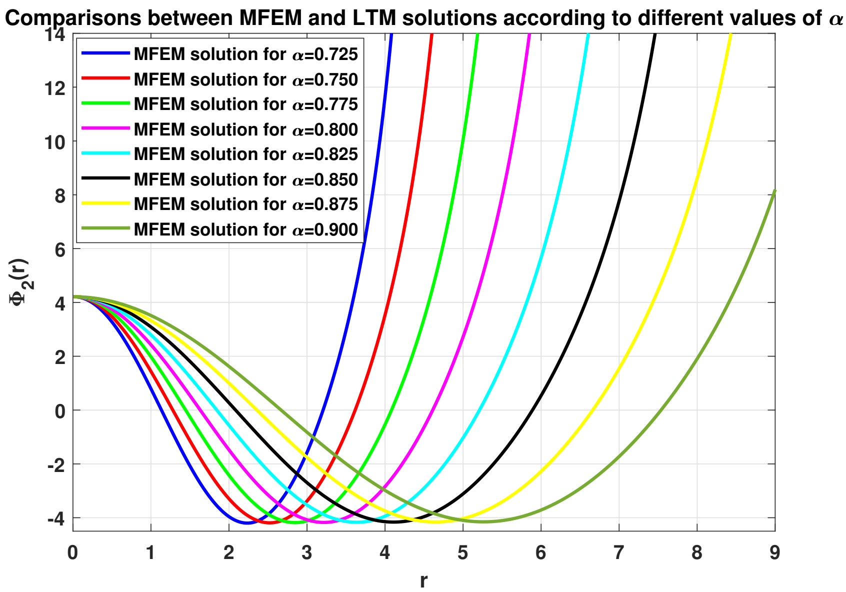

Figure 21: MFEM's solutions of $\phi_2(r)$ in slab reactor for different values of α.

https://doi.org/10.54216/IJNS.240401
Received: September 25, 2023 Revised: February 19, 2024 Accepted: May 07, 2024

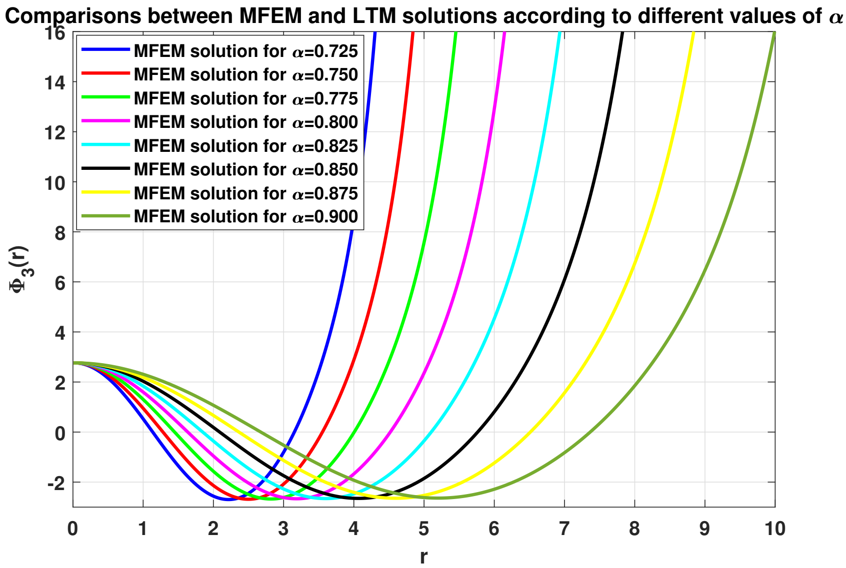

Figure 22: MFEM's solutions of $\phi_3(r)$ in slab reactor for different values of α.

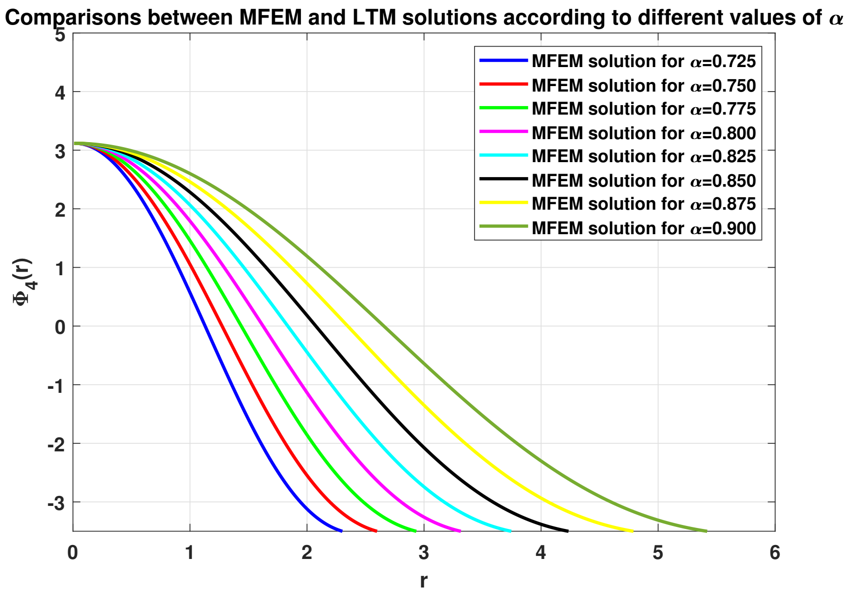

Figure 23: MFEM's solutions of $\phi_4(r)$ in slab reactor for different values of α.

https://doi.org/10.54216/IJNS.240401

Received: September 25, 2023 Revised: February 19, 2024 Accepted: May 07, 2024

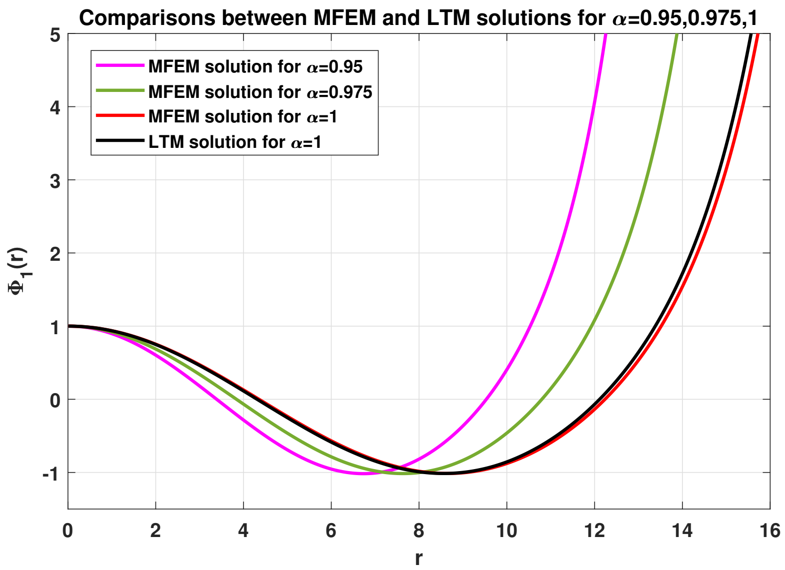

Figure 24: LTM's and MFEM's solutions of $\phi_1(r)$ in slab reactor for $\alpha = 0.95, 0.975, 1$.

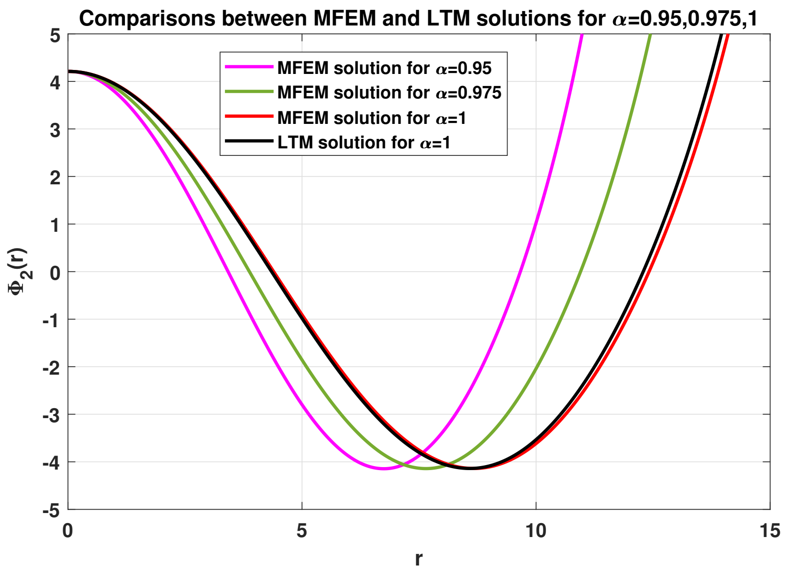

Figure 25: LTM's and MFEM's solutions of $\phi_2(r)$ in slab reactor for $\alpha = 0.95, 0.975, 1$.

https://doi.org/10.54216/IJNS.240401

Received: September 25, 2023 Revised: February 19, 2024 Accepted: May 07, 2024

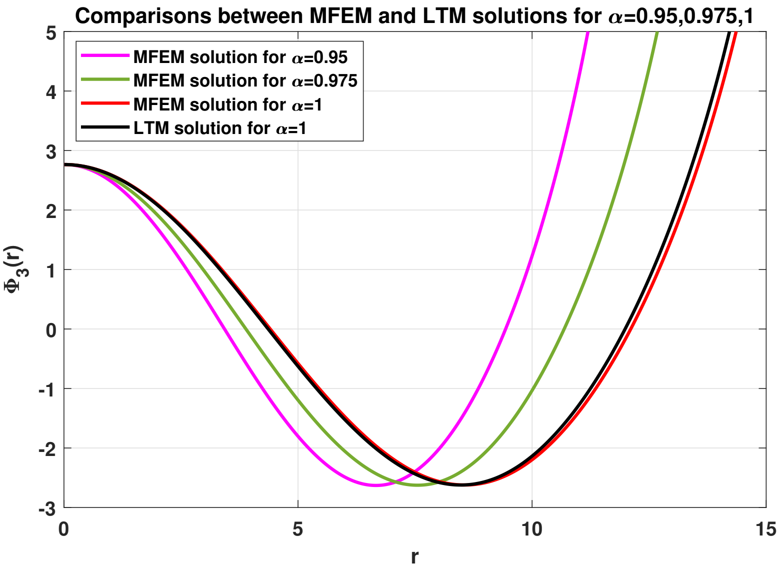

Figure 26: LTM's and MFEM's solutions of $\phi_3(r)$ in slab reactor for $\alpha = 0.95, 0.975, 1$.

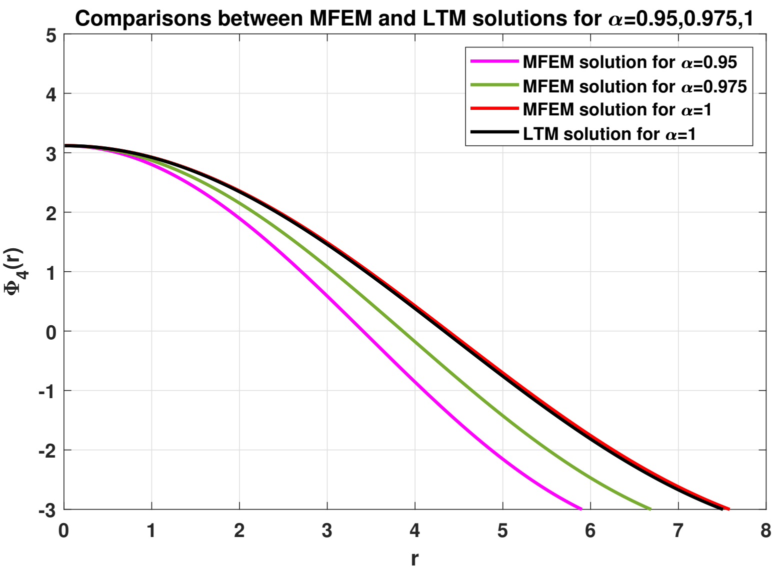

Figure 27: LTM's and MFEM's solutions of $\phi_3(r)$ in slab reactor for $\alpha = 0.95, 0.975, 1$.

https://doi.org/10.54216/IJNS.240401
Received: September 25, 2023 Revised: February 19, 2024 Accepted: May 07, 2024

6 Conclusion

In this study, two numerical solutions to multi-group neutron diffusion systems of equations with fractional-order values have been discussed. First, it has solved the multi-group neutron diffusion equations in their classical form using the Laplace transform method. It has then used the Caputo differentiator to convert these equations into their equivalent fractional-order cases. A innovative strategy has been introduced to reduce the resulting fractional-order system from a system of 2α-order to a system of α-order in order to manage it. The so-called modified fractional Euler method has subsequently been applied to solve this modified system. The multi-group neutron diffusion equations in slab, spherical, and cylindrical reactors have been covered in the work.

References

[1] M. A. Shafii, I. Zakiya, D. Fitriyani, S. H. J. Tongkukut, A. G. Abdulla, Characteristics of neutron diffusion coefficient as a function of energy group in the one-dimensional multi-group diffusion equation of finite slab reactor core, Journal of Physics: Conference Series, vol. 1869, 012202, 2021.

[2] T. Sardar, S. Saha Ray, R. K. Bera, The solution of coupled fractional neutron diffusion equations with delayed neutrons, International Journal of Nuclear Energy Science and Technology, vol. 5, no. 2, pp. 105–133, 2010.

[3] A. S. Kochenov, The stability of a nuclear power plant, Journal of Nuclear Energy. Part A. Reactor Science, vol. 12, no. 4, pp. 194-200, 1960.

[4] S. Dababneh, K. Khasawneh, Z. Odibat, An alternative solution of the neutron diffusion equation in cylindrical symmetry, Ann. Nucl. Energy, vol. 38, pp. 1140–1143, 2010.

[5] M. Shqair, Developing a new approaching technique of homotopy perturbation method to solve two-group reflected cylindrical reactor, Results Phys., vol. 12, pp. 1880–1887, 2019.

[6] M. Shqair, E. A. Farrag, M. Al-Smadi, Solving multi-group reflected spherical reactor system of equations using the homotopy perturbation method, Mathematics, vol. 10, no. 10, 1784, 2022.

[7] M. Shqair, I. Ghabar, A. Burqan, Using Laplace residual power series method in solving coupled fractional neutron diffusion equations with delayed neutrons system, Fractal Fract., vol. 7, 219, 2023.

[8] S. Khaled, Exact solution of the one-dimensional neutron diffusion kinetic equation with one delayed precursor concentration in Cartesian geometry, AIMS Math., vol. 7, pp. 12364–12373, 2022.

[9] T. Sardar, S. Ray, R. Bera, The solution of coupled fractional neutron diffusion equations with delayed neutrons, Int. J. Nuclear Energy Sci. Technol., vol. 5, pp. 105–133, 2010.

[10] R. A. El-Nabulsi, Nonlocal effects to neutron diffusion equation in a nuclear reactor, Journal of Computational and Theoretical Transport, vol. 49, no. 6, pp. 267-281, 2020.

[11] R. A. El-Nabulsi, Neutrons diffusion variable coefficient advection in nuclear reactors, International Journal of Advanced Nuclear Reactor Design and Technology, vol. 3, pp. 102-107, 2021.

[12] S. Ray, A. Patra, Application of homotopy analysis method and Adomian decomposition method for the solution of neutron diffusion equation in the hemisphere and cylindrical reactors, Journal of Nuclear Engineering and Technology, vol. 1, pp. 1–14, 2011.

[13] A. Nahla, F. Al-Malki, M. Rokaya, Numerical Techniques for the Neutron Diffusion Equations in the Nuclear Reactors, Adv. Studies Theor. Phys., vol. 6, pp. 649–664, 2012.

[14] S. M. Khaled, Exact solution of the one-dimensional neutron diffusion kinetic equation with one delayed precursor concentration in Cartesian geometry, AIMS Mathematics, vol. 7, no. 7, pp. 12364-12373, 2022.

[15] J. S. Cassell, M. M. R. Williams, A solution of the neutron diffusion equation for a hemisphere with mixed boundary conditions, Annals of Nuclear Energy, vol. 31, pp. 1987–2004, 2004.

https://doi.org/10.54216/IJNS.240401
Received: September 25, 2023 Revised: February 19, 2024 Accepted: May 07, 2024

[16] K. Khasawneh, S. Dababneh, Z. Odibat, A solution of the neutron diffusion equation in hemispherical symmetry using the homotopy perturbation method, Annals of Nuclear Energy, vol. 36, pp. 1711-1717, 2009.

[17] A. Sood, R. Forster, D. Parsons, Analytical Benchmark Test Set for Criticality Code Verification, Los Alamos National Laboratory, 1999.

[18] A. Burqan, M. Shqair, A. El-Ajou, S. M. E. Ismaeel, Z. Al-Zhour, Analytical solutions to the coupled fractional neutron diffusion equations with delayed neutrons system using Laplace transform method, AIMS Mathematics, vol. 8, no. 8, pp. 19297–19312, 2023.

[19] M. Shqair, I. Ghabar, A. Burqan, Using Laplace residual power series method in solving coupled fractional neutron diffusion equations with delayed neutrons system, Fractal Fract., vol. 7, 219, 2023.

[20] J. J. Duderstadt, L. J. Hamilton, Nuclear Reactor Analysis, John Wiley, Sons, 1976.

[21] J. R. Lamarsh, Introduction to Nuclear Engineering, Addison-Wesley, 1983.

[22] M. Nairat, M. Shqair, T. Alhalholy, Cylindrically symmetric fractional Helmholtz equation, Appl. Math. E-Notes, vol. 19, pp. 708-717, 2019.

[23] I. M. Batiha, A. Bataihah, A. Al-Nana, S. Alshorm, I. H. Jebril, A. Zraiqat, A numerical scheme for dealing with fractional initial value problem, International Journal of Innovative Computing, Information and Control, vol. 19, no. 3, pp. 763-774, 2023.

[24] I. M. Batiha, S. Alshorm, I. H. Jebril, M. A. Hammad, A brief review about fractional calculus, Int. J. Open Problems Compt. Math., vol. 15, no. 4, pp. 39-56, 2022.

[25] I. M. Batiha, S. Alshorm, A. Al-Husban, R. Saadeh, G. Gharib, S. Momani, The n-point composite fractional formula for approximating Riemann–Liouville integrator, Symmetry, vol. 15, no. 4, 938, 2023.

[26] T. Hamadneh, A. Abbes, I. Abu Falahah, Y. A. AL-Khassawneh, A. S. Heilat, A. Al-Husban, A. Ouannas, Complexity and chaos analysis for two-dimensional discrete-time predator–prey Leslie–Gower model with fractional orders, Axioms, vol. 12, no. 6, 561, 2023.

[27] I. M. Batiha, Z. Chebana, T. Oussaeif, A. Ouannas, S. Alshorm, A. Zraiqat, Solvability and dynamics of superlinear reaction diffusion problem with integral condition, IAENG International Journal of Applied Mathematics, vol. 53, no. 1, pp. 1-9, 2023.

[28] A. Dababneh, A. Zraiqat, A. Farah, H. Al-Zoubi, M. Abu Hammad, Numerical methods for finding periodic solutions of ordinary differential equations with strong nonlinearity, J. Math. Comput. Sci., vol. 11, no. 6, pp. 6910-6922, 2021.

[29] I. M. Batiha, A. Benguesmia, T. E. Oussaeif, I. H. Jebril, A. Ouannas, S. Momani, Study of a superlinear problem for a time fractional parabolic equation under integral over-determination condition, IAENG International Journal of Applied Mathematics, vol. 54, no. 2, pp. 187-193, 2024.

[30] I. M. Batiha, N. Allouch, I. H. Jebril, S. Momani, A robust scheme for reduction of higher fractional-order systems, Journal of Engineering Mathematics, vol. 144, no. 1, 4, 2024.

[31] I. M. Batiha, I. H. Jebril, S. Alshorm, M. Aljazzazi, S. Alkhazaleh, Numerical approach for solving incommensurate higher-order fractional differential equations, Nonlinear Dynamics and Systems Theory, vol. 24, no. 2, 123, 2024.

[32] I. M. Batiha, I. H. Jebril, S. Alshorm, A. A. Al-Nana, S. Alkhazaleh, S. Momani, Handling systems of fractional stochastic differential equations using modified fractional Euler method, Global & Stochastic Analysis, vol. 11, no. 1, pp. 95-105, 2024.

[33] A. A. Kilbas, Theory and Application of Fractional Differential Equations, Elsevier, Amsterdam, 2006.

[34] L. Beghina, M. Caputo, Commutative and associative properties of the Caputo fractional derivative and its generalizing convolution operator, Commun. Nonlinear Sci. Numer. Simulat., vol. 89, 105338, 2020.

[35] Z. M. Odibat, S. Momani, An algorithm for the numerical solution of differential equations of fractional order, Journal of Applied Mathematics & Informatics, vol. 26, no. 1-2, pp. 15-27, 2008.

https://doi.org/10.54216/IJNS.240401
Received: September 25, 2023 Revised: February 19, 2024 Accepted: May 07, 2024

[36] J. L. Schiff, The Laplace Transform: Theory and Applications, Springer-Verlag, New York Inc, 1999.

https://doi.org/10.54216/IJNS.240401
Received: September 25, 2023 Revised: February 19, 2024 Accepted: May 07, 2024